

1 **TITLE: Climate change reduces resilience to fire in subalpine rainforests**

2 **Running head: Climate change effects on forest resilience**

3 Michela Mariani*^{1,2}, Michael-Shawn Fletcher*¹, Simon Haberle³, Hahjung Chin³, Zawadzki, A.⁴,
4 Geraldine Jacobsen⁴

5

6 ¹School of Geography, University of Melbourne, VIC, Australia

7 ² School of Geography, University of Nottingham, Nottingham, United Kingdom³ Department of
8 Archaeology and Natural History, Australian National University, ACT, Australia⁴ Australian Nuclear
9 Science and Technology Organisation (ANSTO), NSW, Australia

10

11 *Corresponding authors: michela.mariani@nottingham.ac.uk, +44 7706478298;

12 michael.fletcher@unimelb.edu.au, +61 390353048

13

14 Paper type: Primary Research Article

15

16 **ABSTRACT**

17 Climate change is affecting the distribution of species and the functioning of ecosystems. For
18 species that are slow growing and poorly dispersed, climate change can force a lag between the
19 distributions of species and the geographic distributions of their climatic envelopes, exposing
20 species to the risk of extinction. Climate also governs the resilience of species and ecosystems
21 to disturbance, such as wildfire. Here we use species distribution modelling and palaeoecology
22 to assess and test the impact of vegetation-climate disequilibrium on the resilience of an

23 endangered fire-sensitive rainforest community to fires. First, we modelled the probability of
24 occurrence of *Athrotaxis* spp. and *Nothofagus gunnii* rainforest in Tasmania (hereon ‘montane
25 rainforest’) as a function of climate.. We then analysed three pollen and charcoal records
26 spanning the last 7500 cal yr BP from within both high (n=1) and low (n=2) probability of
27 occurrence areas. Our study indicates that climatic change between 3000 and 4000 cal yr BP
28 induced a disequilibrium between montane rainforests and climate that drove a loss of
29 resilience of these communities. Current and future climate change are likely to shift the
30 geographic distribution of the climatic envelopes of this plant community further, suggesting
31 that current high resilience locations will face a reduction in resilience. Coupled with the
32 forecast of increasing fire activity in southern temperate regions, this heralds a significant threat
33 to this and other slow growing, poorly dispersed and fire sensitive forest systems that are
34 common in the southern mid- to high latitudes.

35

36 **1. INTRODUCTION**

37 Climate exerts a first order control over the functioning and distribution of species and
38 ecosystems on Earth. Under current global climate projections, ecosystems are experiencing
39 increased climatic pressures that alter their function and their provisioning of services to society
40 (Milliennium Ecosystem Assessment, 2005). The rate of recent climatic change exceeds any
41 period inferred from historic and geological records and the potential of organisms to adapt to
42 these changes is poorly understood (Burrows *et al.*, 2014). Compounding the effects of climate
43 change on ecosystem dynamics is the impact of disturbance events. Climatic change represents
44 a ‘press’ perturbation on biological systems that can act synergistically with discrete extreme
45 events (‘pulse’ disturbances), such as wildfires, bark beetles infestations or windstorms (Seidl
46 *et al.*, 2014, Seidl *et al.*, 2016). Indeed, a number of recent ecosystem collapses have occurred
47 in response to the loss of ecosystem resilience resulting from recent climate change and its

48 impact on the ability of ecosystem to recover from extreme events (Harris *et al.*, 2018). Here,
49 we use species distribution modelling and palaeoecology to assess and test the influence of
50 long-term climate change on the ecological resilience to disturbance from fire of the UNESCO-
51 listed and endangered temperate montane rainforests in Tasmania, Australia.

52

53 Climate change over the last century is already affecting resilience and distribution of species
54 (Bateman *et al.*, 2016, Chen *et al.*, 2011, Hirota *et al.*, 2011, Lenoir & Svenning, 2015,
55 Parmesan, 2006, Parmesan & Yohe, 2003). Amongst all ecosystems, mountains and their
56 unique biota are the most exposed to climate and land-use change (Guo *et al.*, 2018), given the
57 accentuation of climatic change by elevation and the diminishing area of land available upslope
58 in most settings (Beniston, 2003, Nogués-Bravo *et al.*, 2007, Theurillat & Guisan, 2001). The
59 montane rainforests located in the topographically complex landscape of Tasmania have a
60 canopy dominated by long-lived (500-1500 years) tree species that are slow-growing, poorly
61 dispersed and highly sensitive to disturbance from fire (Cullen, 1987). Longevity, poor
62 dispersal and complex topography facilitate the persistence of ecosystems *in situ* following
63 climate change, resulting in an increase in the potential for disequilibrium between ecosystems
64 and climate (Lenoir *et al.*, 2013, Loehle, 2018). Resilience to disturbance events varies in
65 response to climate (Beever & Belant, 2011, Crimmins *et al.*, 2011, Hirota *et al.*, 2011,
66 VanDerWal *et al.*, 2013), with a shift toward less favourable climate conditions associated with
67 a reduction in the rate of growth, recovery and reproduction of tree species following
68 disturbance (Enright *et al.*, 2015). Thus, shifts in climate space following climatic changes may
69 decrease the capacity of ecosystems to respond to disturbance, placing them at risk of loss and
70 potential extinction.

71

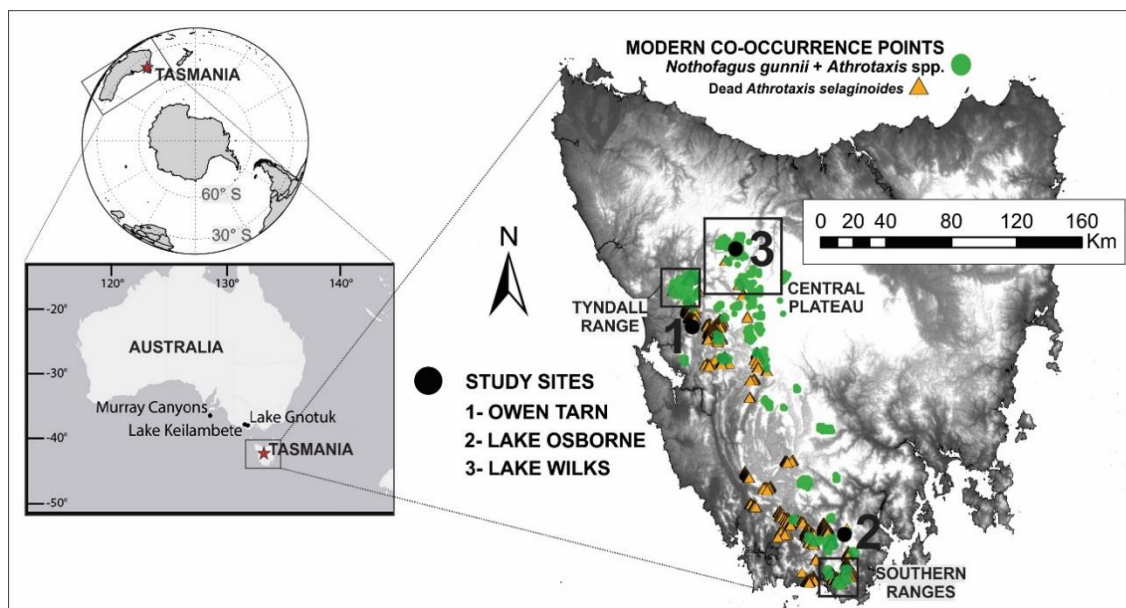
72 Wildfires are one of the most important disturbance types within terrestrial vegetation (Bond
73 *et al.*, 2005, Bowman *et al.*, 2009), and are particularly important in the Australian landscape
74 (Hennessy *et al.*, 2005). Recent climate change has intensified fire weather severity worldwide
75 (Aldersley *et al.*, 2011) which, coupled with a lengthening of fire seasons, has resulted in both
76 an increase in ‘mega-fires’ (Stephens *et al.*, 2014, Westerling *et al.*, 2006) and an increase in
77 the occurrence of lightning-ignited fires (Mariani *et al.*, 2018, Styger *et al.*, 2018). In this context
78 of changing fire regimes, promoting the resilience of fire-sensitive species and reducing the
79 risk of extinction is a crucial task for modern-day ecosystem managers (Seidl *et al.*, 2014, Seidl
80 *et al.*, 2016). This objective is especially challenging in ecosystems featuring long-lived plant
81 species, as historical records (spanning the last decades) are too short for us to understand the
82 full range of variability of these organisms and how adaptable they are to climatic change
83 (Birks *et al.*, 2016, Willis & Birks, 2006). Thus, to adequately manage ecosystems, the
84 projection of magnitude and direction of environmental changes should be understood in the
85 context of the long-term history of key species within the ecosystem of interest.

86

87 In this paper we take advantage of the well-studied long-term climatic history of Tasmania
88 through the last 7500 years, which indicates a shift from a stable wet climate to a variable and
89 overall drier climate between 3000 and 4000 cal yr BP, to assess and test how climatic change
90 influences the resilience of montane rainforest in Tasmania to fire. We use species distribution
91 modelling to estimate the probability of co-occurrence of two key montane rainforest tree taxa
92 (*Athrotaxis* spp. and *Nothofagus gunnii*) as a function of climate. We then use palaeoecology
93 to reconstruct montane rainforest and fire histories over the past 7500 years from sites of high
94 probability of occurrence (Lake Wilks) and low probability of occurrence (Lake Osborne and
95 Owen Tarn) in an attempt to understand the process of montane rainforest recovery from fire
96 disturbance under varying climatic contexts (Fig. 1c, Fig. 2). We predict that a combination of

107 the extreme longevity of key species in this system (>1000 years), landscape heterogeneity and
108 long-term climatic change will have created a situation in which stands of this highly
109 fragmented forest type are either at the limits of their climatic range or in disequilibrium with
110 climate. Thus, we predict that the probability of occurrence produced by our climate-based
111 species distribution model will provide a good approximation of the climate equilibrium state
112 of existing montane rainforest stands in Tasmania, which, in turn, will provide an indication of
113 the potential resilience of this forest type to disturbance from fire (*sensu* Hirota *et al.*, 2001).
114 We hypothesize that sites with a low probability of occurrence will display a reduced resilience
115 to disturbance from fire and sites with a high probability of occurrence will display a higher
116 degree of resilience disturbance from fire disturbance (i.e. high resilience).

107



108

109 **Fig. 1** Map showing the location of modern co-occurrence of *Nothofagus gunnii* and *Athrotaxis*
110 spp. (i.e. montane rainforest, green dots) and location of dead *Athrotaxis selaginoides* patches
111 (orange triangles, data from TasVeg3.0 – Government of Tasmania, 2013). Black dots
112 represent the study sites for the long-term charcoal and pollen analyses: 1-Owen Tarn (OT), 2-
113 Lake Osborne (LO) and 3-Lake Wilks (LW).

114

115

116 2. MATERIAL AND METHODS

117 2.1 Study Area

118 Fire and montane rainforests in Tasmania

119 Today, *Athrotaxis* spp.-*N. gunnii* montane rainforests cover <5% of the Tasmanian landscape,
120 mostly as small pockets of forest confined to the Central Plateau, the Tyndall Range and
121 scattered mountain tops in the southwest (Fig. 1a). These species, and related rainforest taxa,
122 were more widespread across Tasmania and continental Australia during the Cainozoic, a part
123 of the so-called Gondwanan flora that dominated the southern latitudes (Hill, 1991). The
124 modern-day restricted distribution of these species has resulted from a combination of
125 increasing aridity, fire and the radiation of fire-adapted and fire-promoting plant taxa through
126 the Cainozoic to present (Bowman, 2000). Humans colonised Tasmania during the Last Glacial
127 Cycle (>40,000 years ago) (Cosgrove, 1999) imparting a substantial imprint on the vegetation
128 landscape through the use of fine-scale fire management that further restricted the distribution
129 of fire-sensitive plants (Fletcher & Thomas, 2010, Mariani *et al.*, 2017). Today, treeless
130 pyrophytic vegetation dominates the landscape (including *Gymnoschoenus sphaerocephalus*
131 and species of *Melaleuca* and *Leptospermum*), with fire-sensitive arboreal communities largely
132 restricted to topographic fire refugia in Tasmania's west and south (Wood *et al.*, 2011). Key
133 among the fire sensitive communities are the iconic and now endangered montane rainforests.
134 Montane rainforest in Tasmania forms at high elevation (ca. 700-1000 m a.s.l.) and is
135 dominated by endemic tree species, such as the UNESCO heritage-listed trees, *Athrotaxis*
136 *cupressoides*, *A. selaginoides* and *Nothofagus gunnii* (syn. *Fuscospora gunnii*) (Harris &
137 Kitchener, 2005). Here, we retain use of *Nothofagus* to maintain consistency with fossil records
138 (*sensu* Hill *et al.*, 2015).

139

140 *Athrotaxis* spp. and *N. gunnii* display several life history attributes that suggest they are poorly
141 adapted to disturbance by fire: (1) they are long lived (>1000 years for *Athrotaxis* spp.; >500
142 years for *N. gunnii*) and slow-growing (Allen *et al.*, 2011, Ogden, 1978); (2) they are obligate
143 seeders that display almost complete stand-scale mortality following fire (Cullen, 1987, Cullen
144 & Kirkpatrick, 1988, Kirkpatrick & Dickinson, 1984); (3) they display an apparent post-fire
145 regeneration failure following moderate to severe fire events that indicates low post-fire soil
146 seedbank survivorship (Holz *et al.*, 2014, Kirkpatrick & Dickinson, 1984); and (4) they have
147 relatively large and poorly dispersed seeds, which are often produced at irregular, supra-annual
148 intervals (Calais & Kirkpatrick, 1983, Cullen, 1987). Despite the apparent hyper-sensitivity
149 and poor adaptation to fire, slow (>800 years) post-fire recovery of montane rainforest is
150 evident in the palaeoecological record (Fletcher *et al.*, 2014, 2018; Cadd *et al.*, in review), with
151 fire-driven elimination of this community considered a product of decreased resilience in
152 response to repeated and more frequent burning and a shift to a climate less hospitable to the
153 post-fire regeneration and growth of montane rainforest species through the Holocene (Fletcher
154 *et al.*, 2014, 2018).

155

156 Importantly, it is unclear whether the loss of resilience to disturbance from fire in montane
157 rainforest is solely the product of a synergistic interaction between the effects of repeated
158 burning and climatic change, or whether climatic change alone is sufficient to reduce the
159 capacity of this plant community to respond to fire. Both *Athrotaxis* spp. and *N. gunnii* have
160 suffered major fire-driven landscape-scale losses across their entire range over the last 200
161 years (the post-colonial period) (Brown, 1988, Cullen, 1991, Holz *et al.*, 2014, Kirkpatrick &
162 Dickinson, 1984), with an estimated fire-driven range reduction of >30% for *Athrotaxis* in this
163 time (Brown, 1988; Figure 1a). To date, no post-fire recovery of these stands has been

164 observed. It is unclear whether this is the result of 1) an insufficient recovery window following
165 fires or 2) the underlying press of climate change now precludes the recovery of these species
166 to fire (pulse) disturbance. This knowledge is critical for the long-term management of montane
167 rainforest under current and predicted trends in climate and fire regimes. A case-in-point is the
168 catastrophic landscape-scale 2016 wildfires that decimated the largest remaining patch of *A.*
169 *cupressoides* vegetation in Tasmania (Harris et al., 2018). Future-proofing these systems from
170 fire in the remote Tasmanian landscape requires enormous financial and logistical resourcing
171 and there is an urgent need to understand the relative roles of the various factors that influence
172 resilience to fire of these systems, such as fire history and climatic change, to guide effective
173 and efficient environmental management.

174

175 **Climate variability in Tasmania over the last 7500 years**

176 Overall, the extensive palaeoclimate data from the region indicates an early high moisture
177 period with a broadly stable temperature regime between ca. 7500-4000 cal yr BP, with a shift
178 toward a more variable moisture and temperature regime after 4000 cal yr BP. There is a
179 general agreement that the period between 7500 cal yr BP and 4000 cal yr BP (mid-Holocene)
180 was relatively wet across the southeast sector of southern Australia as a consequence of an
181 increase in precipitation delivered by a stronger zonal circulation (see Fletcher & Moreno,
182 2012, Mariani & Fletcher, 2017, and references therein) (Fig. 3d). Temperatures are thought
183 to have been relatively stable through this period (Marcott et al., 2013), although sea-surface
184 temperatures (SST) in the region suggest a decline in temperature from a Holocene optimum
185 at ca. 7500 cal yr BP (Calvo *et al.*, 2007). In contrast, the late Holocene (ca. 4000 cal yr BP –
186 present) was characterised by a shift toward a more variable and overall drier moisture regime
187 over Tasmania and surrounding areas (Mariani & Fletcher, 2017, Rees *et al.*, 2015, Stahle *et*
188 *al.*, 2017, Xia *et al.*, 2001), likely in response to the onset of ENSO-like climate variability in

189 the Pacific region leading to more frequent El Niño (dry) phases (Donders *et al.*, 2008, Fletcher
190 & Moreno, 2012), which drove an increase in wildfire across Tasmania (Fletcher *et al.*, 2015,
191 Mariani & Fletcher, 2017)(Fig. 3d). Estimates of temperature change though this period
192 indicate high variability (Marcott *et al.*, 2013)(Fig. 3e), while SSTs in the region suggest a
193 continued decline toward the present (Calvo *et al.*, 2007).

194

195 **Study sites**

196 Owen Tarn (1-OT; 42.0998S, 145.6094E; 970 m a.s.l.) is a small subalpine lake, located on the
197 eastern flank of Mount Owen (1,146 m a.s.l.) in central western Tasmania. Total annual rainfall
198 is 2804 mm/yr and the annual mean temperature is 8.4°C. Today, the lake catchment is mostly
199 characterised by exposed bedrock and small patches of western subalpine scrub (including
200 *Leptospermum nitidum*, *Eucalyptus vernicosa*, *Monotoca submutica*, *Agastachys odorata* and
201 *Cenarrhenes nitida*). The presence of tree stumps in the catchment indicate that the lake was
202 formerly more densely vegetated (Hodgson *et al.*, 2000), but no individuals of montane
203 rainforest trees occur today.

204

205 Lake Osborne (2-LO; 43.2159S, 146.7589E; 924 m a.s.l.) is a small moraine-bound subalpine
206 lake, located in the Hartz Ranges in southwest Tasmania. Total annual rainfall at the closest
207 meteorological station is 1443 mm/yr and the annual mean temperature is 9.7°C. Dominant
208 species in the modern landscape are *Eucalyptus coccifera*, *Nothofagus cunninghamii* (syn.
209 *Lophozonia cunninghamii*), *Eucryphia milliganii*, *Gahnia grandis* and a variety of Protaceae
210 shrubs. Only a few fire-scarred individuals of *Athrotaxis selaginoides* are growing on the shore
211 of the lake, although no living individuals are present around the catchment.

212

213 Lake Wilks (3-LW; 41.6729S, 145.9552E; 1060 m a.s.l.) is a small cirque lake located in
 214 UNESCO World Heritage Area in northwest Tasmania. Total annual rainfall is 2832 mm/yr
 215 and the annual mean temperature is 8.3°C. The present-day catchment of Lake Wilks is mostly
 216 occupied by *Athrotaxis-N. gunnii* rainforest.

217 A summary of the information on the three sites used for the analyses presented in this work
 218 is shown in Table 1.

219

220

221

222

223 **Table 1** Summary information of the sites used for the long-term analyses in this work.

224 Asterisks (*) indicates extrapolated values from BIOCLIM predictor layers (Fig. S1).

Site code	1	2	3	
Site Name	Owen Tarn	Lake Osborne	Lake Wilks	
Latitude °S	-41.451196	-42.099683	-41.672829	
Longitude °E	145.961463	145.609434	145.956023	
Elevation	969	920	1058	
Temperature of the warmest quarter (°C) - bio10	11.8	10.9	9.3	
Precipitation of the warmest quarter (mm) - bio18	593	234	388	
Temperature seasonality (°C) - bio04	1.03	1.03	1.14	
Precipitation seasonality (%) - bio15	21	17	27	
Modern montane rainforest	NO	NO	YES	
MaxEnt value	0.437	0.301	0.826	
Publications	Charcoal data	Mariani & Fletcher, 2017	Fletcher <i>et al.</i> , 2014; 2018	Stahle <i>et al.</i> , 2017
	Pollen data	This study (partial)	Fletcher <i>et al.</i> , 2014; 2018	This study (partial)
	Chronology			Stahle <i>et al.</i> , 2017

		Mariani & Fletcher, 2017 (updated in this study)	Fletcher <i>et al.</i> , 2014; 2018	
--	--	--	--	--

225

226

227

228 **2.2 Species distribution modelling**

229 We used the MaxEnt v3.3.3k program (Phillips *et al.*, 2004) implemented into R (R Core
230 Development Team, 2013) and the *dismo* package (Hijmans *et al.*, 2017) to model the
231 probability of occurrence of montane rainforest across Tasmania as a function of climate. The
232 MaxEnt algorithm is designed for species distribution modelling using a set of environmental
233 variables (Phillips *et al.*, 2004) and it was found to be more conservative than other models in
234 predicting probability of species occurrence (Kumar *et al.*, 2009, Kumar & Stohlgren, 2009).
235 This algorithm uses presence and pseudo-absence or background data of the variable of interest
236 (i.e. species distribution) to compare the values of the environmental predictors associated with
237 these presence points with those of a background (or pseudo-absence localities). This approach
238 estimates the “maximum entropy” of sampling points compared to background locations, by
239 taking into account the constraints derived from the predictor variables (Baldwin, 2009,
240 Phillips *et al.*, 2004).

241

242 The probability of montane rainforest occurrence was modelled using the modern co-
243 occurrence of *Athrotaxis* spp. and *Nothofagus gunnii* (757 data points) for 500 iterations. The
244 two species were considered co-occurring if located within 1 km distance between each other.
245 A total number of 10000 pseudo-absences (Barbet-Massin *et al.*, 2012) from the convex hull
246 of the presence data were used for the MaxEnt runs to account for dispersal limitations of the
247 chosen taxa (Fig. S1). Presence and pseudo-absence points were divided into two equal groups
248 to create training and testing datasets. Spatial analyses were undertaken using ArcGIS 10.4
249 (ESRI). Four BIOCLIM predictor variables for temperature and precipitation (bio16, bio10,
250 bio4 and bio15) at 0.01 degrees (ca. 1 km at the equator) resolution were used in this model
251 (see Fig. S2 for climate variables maps). BIOCLIM climate predictors (Booth *et al.*, 2014,

252 Nix, 1986) for Tasmania were derived using ANUCLIM v.6 on the Atlas of Living Australia
253 (<http://www.ala.org.au>). The climatic variables were checked for collinearity (Fig. S2).

254

255 **2.3 Fossil data: coring and chronology**

256 Owen Tarn core was retrieved in 2015 using a Universal corer. The chronology of the OT
257 sediment core is based on a combination of ^{210}Pb and ^{14}C dating techniques. Lead radioisotope
258 activity was determined on six samples using alpha-spectrometry at the Australian Nuclear
259 Science and Technology Organisation (ANSTO) after wet sieving the samples to remove sand
260 particles. Eleven radiocarbon dates were obtained on the OT core at ANSTO and DirectAMS
261 (Bothell, USA). Radiocarbon ages were calibrated to calendar years before present (cal yr BP;
262 1950 CE) using the Southern Hemisphere calibration curve (Hogg *et al.*, 2013). Age-depth
263 modelling was performed using linear interpolation in OxCal 4.2 (Ramsey, 2009).

264

265 A combination of two sediment cores were retrieved from the deepest (10m) point of the Lake
266 Osborne basin in 2011. A total of 11 radiocarbon dates and two ^{210}Pb dates were obtained on
267 these cores and ages were modelled against depth using clam (Blaauw, 2010). Results were
268 recently published in Fletcher *et al.*, 2018.

269

270 Lake Wilks core was obtained in 2000 with a modified Livingstone piston sampler. A total of
271 10 radiocarbon dates were obtained on the LW core and calibrated ages were modelled against
272 depth using clam (Blaauw, 2010). Results from these analyses were previously published in
273 Stahle *et al.*, 2017.

274

275 **2.4 Fossil data: pollen and charcoal analysis**

276 Pollen, spores and microscopic charcoal sample preparation followed the standard procedures
277 (Faegri & Iversen, 1989). Pollen analysis was undertaken on the OT core at 0.5 cm intervals
278 for the top 40 cm and 1 cm intervals for the remaining bottom 30 cm. LO was sampled for
279 pollen at 1 cm increments, while a variable resolution between 2 and 8 cm was used for LW.
280 Relative pollen data were calculated from a basic pollen sum that included at least 300
281 terrestrial pollen grains per sample (excluding wetlands and ferns). Only the combined
282 percentages of montane rainforest tree - *Athrotaxis* spp. and *Nothofagus gunnii* - were used in
283 this study.

284

285 Macroscopic charcoal content was analysed to document the local fire history. A volume of
286 1.25 cm³ was taken at continuous 0.5 cm intervals at OT and LO. Lake Wilks core was sampled
287 at 1.0 cm intervals and 2 cm³ were analysed for charcoal content. Charcoal analysis was
288 performed following the method described by Whitlock & Larsen (2001), involving a sediment
289 digestion in 10% hydrogen peroxide for a week (or 5% Sodium Hypochlorite for two weeks).
290 After digestion, sediment was then sieved using 125- μ m mesh diameter (Whitlock & Larsen,
291 2001) and the residues were counted under a stereomicroscope at 40x magnification. Charcoal
292 concentrations and deposition times were calculated and converted to charcoal accumulation
293 rates (CHAR; particles cm² yr⁻¹).

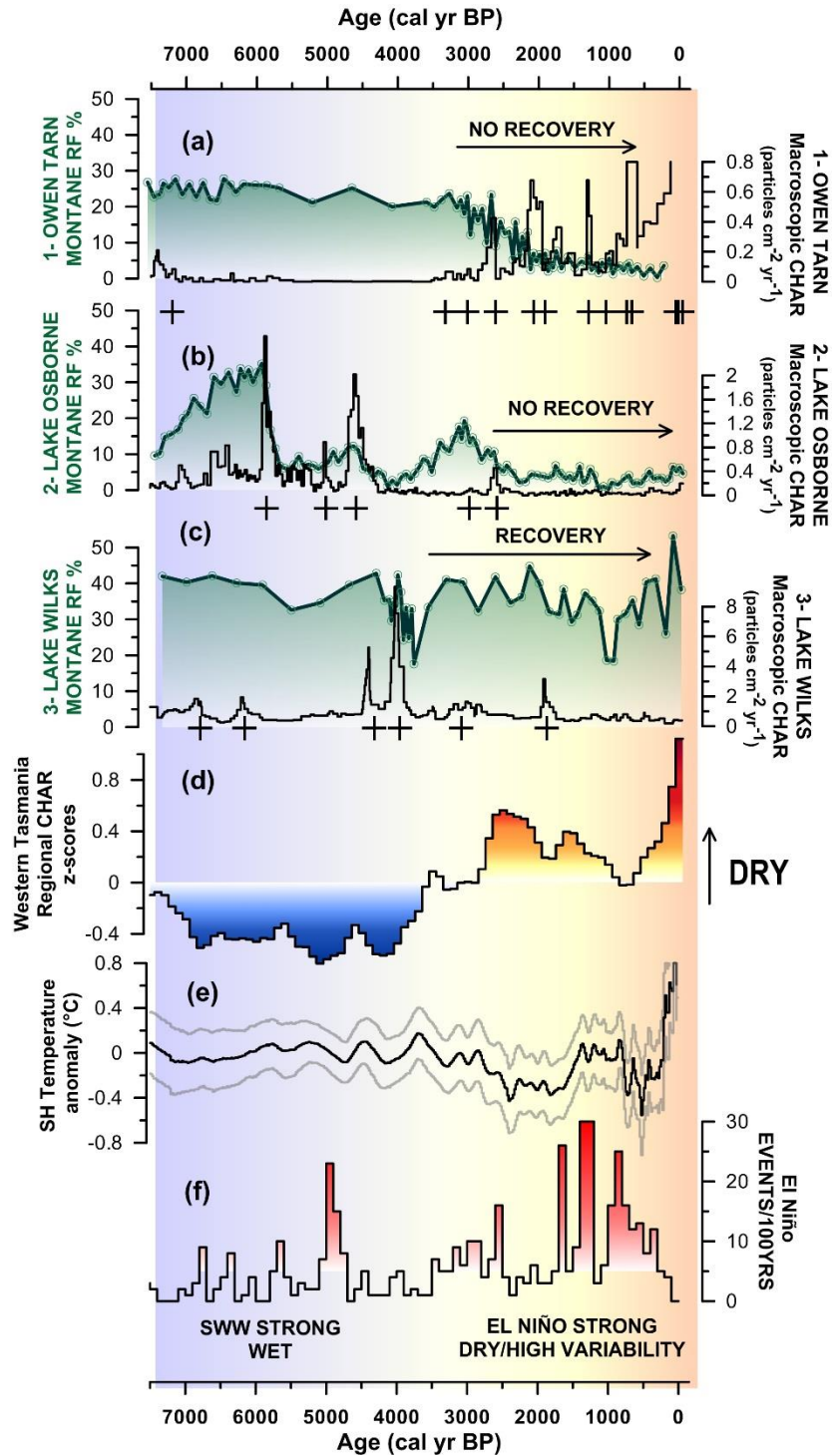
294

295 **2.5 Numerical analyses**

296 Box-and-whiskers plots were used to show the maximum, minimum, the first and third
297 quartiles and median of the montane rainforest pollen data from the three study sites. Two time
298 periods – pre and post 4000 cal yr BP - were chosen based on the reconstructed fire history
299 from these sites and the regional climate changes from regional Tasmania (Mariani & Fletcher,
300 2017). Percentage pollen data were converted to z-scores prior to plotting to reduce skewness

301 due to inter-site differences. Sites located on the ‘edge’ of the climate space (i.e. low resilience
 302 sites) - OT and LO - were combined to simplify the message.

303



304

305 **Fig. 2** Summary plot showing macroscopic charcoal accumulation rates (black line) and
 306 montane rainforest pollen % (green filled curve) spanning the last 7500 cal yr BP from (a)

307 Owen Tarn, (b) Lake Osborne and (c) Lake Wilks (location shown in Fig. 1). Black crosses in
308 (a), (b) and (c) indicate fire events as detected in Figure S11 (OT), Fletcher *et al.*, (2014; LO)
309 and Stahle *et al.* (2017, LW). (d) Regional fire activity reconstruction from western Tasmania
310 (Mariani and Fletcher, 2017). Orange-red fillings in (d) highlight inferred dry periods, whereas
311 shades of blue represent inferred wet phases. (e) Southern Hemisphere temperature stack from
312 Marcott *et al.*, 2013 (black line), grey lines represent the 2σ range. (f) Number of El Niño
313 events/100 years from Laguna Pallcacocha (Moy *et al.*, 2002). Red fillings in (f) represent
314 periods with a frequency of El Niño events higher than five/100 years. The shading from blue
315 to orange indicates the gradual nature of climatic change after 4000 cal yr BP.

316

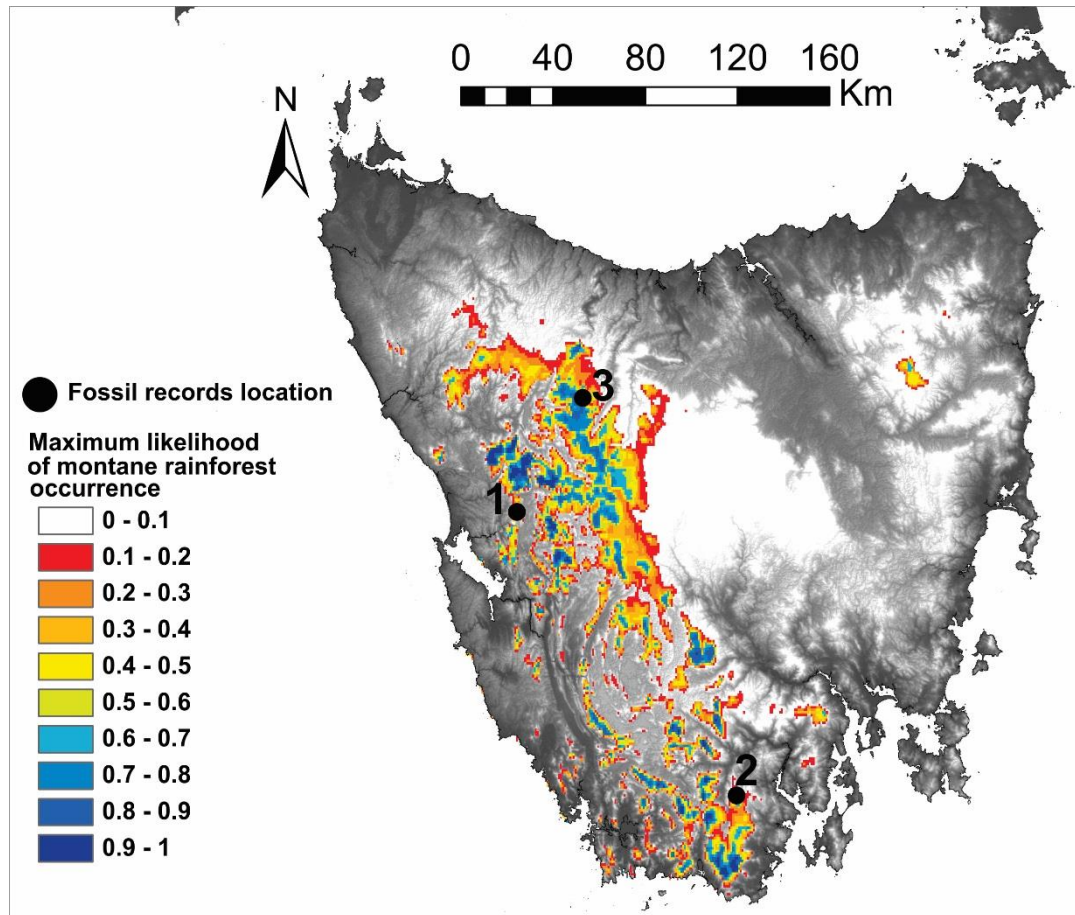
317 **3. RESULTS**

318 **3.1 Modelling species distribution**

319 There was no detectable collinearity amongst the climate predictors used in the MaxEnt model
320 (Fig. S3). The climate variables with the highest percent contribution to the model were the
321 total precipitation and the mean temperature of the warmest quarter (summer season) with an
322 explanatory power of 24% and 72% respectively (Fig. S4), the importance of these variables
323 is as also highlighted in the response curves (Fig. S5, S6). The MaxEnt model was found to
324 perform satisfactorily (AUC=0.877 (training dataset); AUC= 0.853 (testing dataset); random
325 prediction AUC=0.5) when predicting the probability of montane rainforest occurrence based
326 on the four climatic variables (Fig. S7). The MaxEnt model highlighted the areas with the
327 probability of *Athrotaxis* spp. and *N. gunnii* co-occurrence being in the western portion of
328 Tasmania with low annual temperatures of the warmest quarter (mostly $<12^{\circ}\text{C}$) and relatively
329 high precipitation amounts during this period (between 300 and 600 mm; Fig. S8). The highest

330 probability of co-occurrence (>0.5) were found in the Central Plateau, in the Tyndall and in the
331 Southern Ranges (Fig. 2).

332



333

334 **Fig. 3** Map showing the probability of co-occurrence of *N. gunnii* and *Athrotaxis* spp. (i.e.
335 montane rainforest) derived using MaxEnt species modelling (see Material and Methods).
336 Black dots represent the study sites for the long-term charcoal and pollen analyses: 1-Owen
337 Tarn (OT), 2-Lake Osborne (LO) and 3-Lake Wilks (LW).

338

339 3.2 Fossil data: chronology

340 The Owen Tarn record spans the last 7535 cal yr BP over 69 cm (Fig. S9). The list of
341 radiocarbon and ^{210}Pb dates obtained on this core is presented in Table S1a,b. To better
342 constrain the chronology at the bottom of the sequence, the sample at 67.75 cm was dated

343 twice, but a large difference (>1,000 years) was found between the two runs. The older
344 radiocarbon age of 7810 years was considered an outlier due to its impact on the performance
345 of the age-depth model. The oldest radiocarbon age of 6537 years (7401 cal yr BP) was
346 obtained at a depth of 67.75 cm. The age-depth model (Fig. S9) is showing a sigmoid curve,
347 highlighting slower accumulation rates in the mid-section of the core (between 45 and 50 cm)
348 and faster at the bottom and top sections. Accumulation rates were relatively high in the
349 uppermost 17 cm of this sequence (median = 0.14 cm/yr). However, throughout the rest of the
350 sequence, sediment accumulation rates were slow with a median rate of 0.01 cm/yr.

351 The chronologies of LO and LW were previously presented and discussed in Fletcher *et al.*,
352 2018 (LO) and Stahle *et al.*, 2017 (LW), respectively, and age-depth models were presented in
353 Fig. S10. These records extend back to ca. 14000 cal yr BP (LO) and ca. 12000 cal yr BP (LW),
354 however, in this study we only focused on the last 7500 cal yr BP to compare them with the
355 OT record.

356

357 **3.3 Fossil data: pollen and charcoal analysis**

358 A total of 112 samples from OT were analysed for pollen and 138 samples for macroscopic
359 charcoal. The median pollen and charcoal sample resolution is 50 and 49 years, respectively.

360 In this core, montane rainforest pollen showed high abundances between 20-30% through the
361 period from 7500 and 3500 cal yr BP (Fig. 2). A gradual decline in montane rainforest pollen
362 was detected from 3500 cal yr BP up to the British settlement period (ca. 150 cal yr BP). This
363 gradual decrease in the abundance of montane rainforest pollen was concomitant with a
364 persistent increase in macroscopic charcoal (Fig. 2).

365

366 A sum of 118 samples from LO were processed for pollen analysis and a total of 208 samples
367 were analysed for macroscopic charcoal. The median resolution for pollen samples was 64

368 years, whereas the median resolution for charcoal samples was 35 years. Montane rainforest
369 pollen showed three alternating phases of high and low abundances through the period from
370 7500 and 2500 cal yr BP (Fig. 2). The oldest two declines in montane rainforest pollen
371 percentages during this phase clearly coincided with two charcoal peaks (Fig. 2). The third
372 (youngest) decline in montane rainforest percentage (ca. 3000 cal yr BP) occurred slightly prior
373 to the most recent charcoal peak (2700 cal yr BP). In the period between the present and 2500
374 cal yr BP, montane rainforest abundance was maintained below 10%. For more details about
375 pollen and macroscopic charcoal records from LO see Fletcher *et al.*, 2018.

376 Pollen was analysed on 58 samples from the LW core, while macroscopic charcoal was counted
377 on 194 intervals. The median resolution for pollen samples was 83 years, whereas charcoal
378 samples had a median resolution of 44 years. High abundance of montane rainforest pollen was
379 detected throughout the entire sequence with values rarely below 30% (Fig. 2). Around 4000-
380 4500 cal yr BP, a series of two charcoal peaks preceded a long-term decline in montane
381 rainforest pollen percentages down to > 15% at 2700 and 2300 cal yr BP. Hereafter, we use the
382 period between 3000 and 4000 cal yr BP as a boundary of significant change in the records.
383 This reduction is followed by a relatively prompt (<400 years) increase back to the pre-charcoal
384 peak values at ca. 2000 cal yr BP. For more information on the macroscopic charcoal record
385 from Lake Wilks see Stahle *et al.*, (2017).

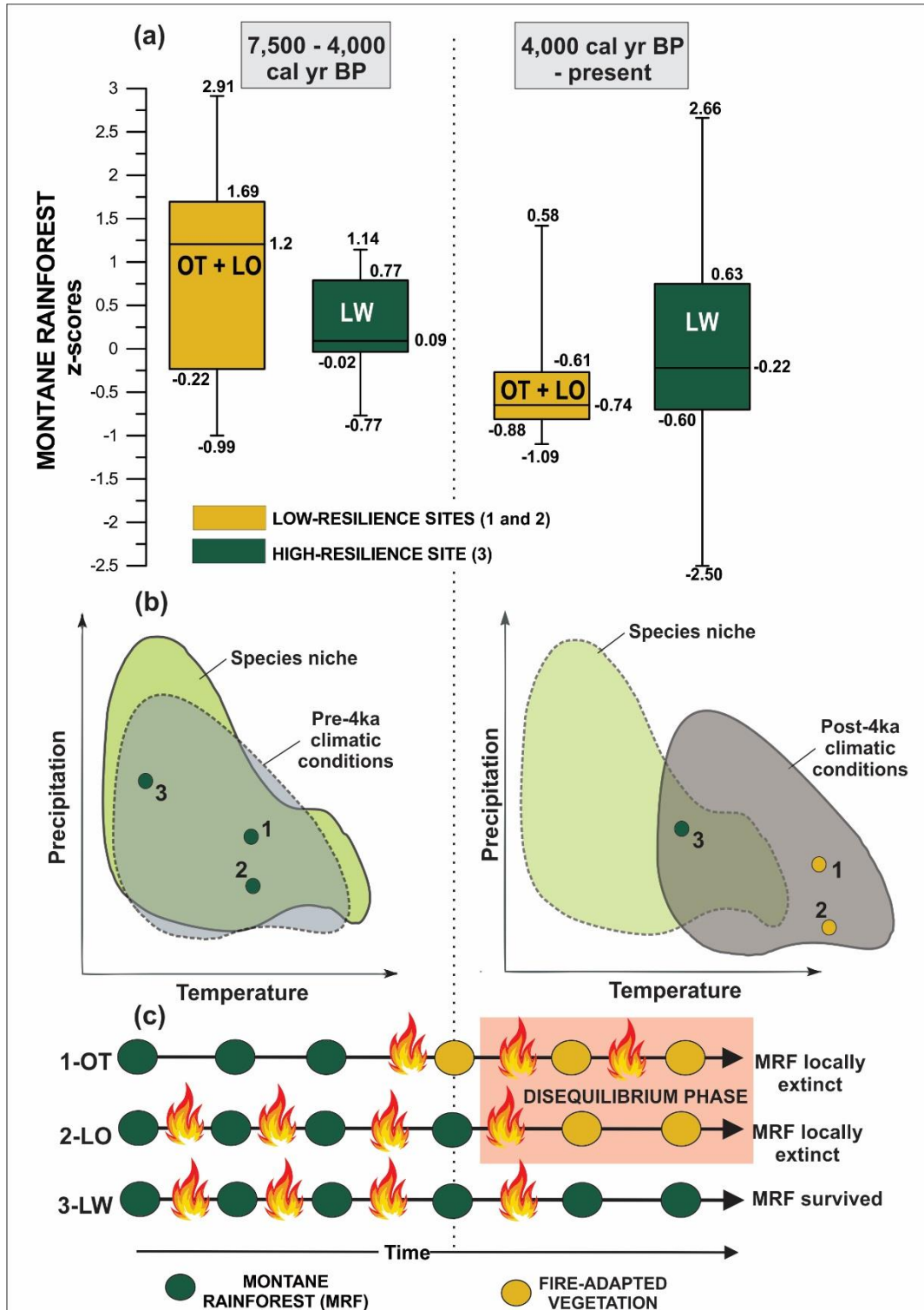
386

387

388 **3.4 Numerical analyses**

389 Box-and-whiskers plots for the period between 7500 and 4000 cal yr BP showed similar
390 montane rainforest data distributions between OT+LO and LW (Fig. 4a, left panel). In both
391 cases, during this phase we observed positive deviations from the mean. Whiskers
392 (representing minimum and maximum values) were substantially shorter in LW in comparison

393 to OT+LO. During the period post-4000 cal yr BP, data distributions diverged, with LW
 394 maintaining a positive median value, while OT+LO show a tight range of values below zero
 395 (Fig. 4a, right panel). Whiskers in LW were broader than OT+LO during this phase.



397 **Fig. 4** a) Box-and-whiskers plots of the normalised montane rainforest pollen abundances (z-
398 scores) from Owen Tarn (OT) + Lake Osborne (LO) and Lake Wilks (LW). Because of the
399 respective position of these lakes in the climate space for montane rainforest, OT and LO are
400 defined as ‘low-resilience sites’ (yellow boxes), while LW is defined as ‘high-resilience site’
401 (green boxes); b) conceptual model depicting a shift in climate space suitable for montane
402 rainforest following the late-Holocene climatic transition in Tasmania (after 4000-3000 cal yr
403 BP). Schematic edited from Ohlemüller *et al.* (2011); c) simplified timeline for the fire and
404 vegetation changes occurred at the three study sites in this work. Red box in c) highlights the
405 disequilibrium phase for OT and LO; MRF = montane rainforest.

406

407 **4. DISCUSSION**

408

409 **4.1 Climate space and montane rainforest resilience**

410 Climate exerts a first-order control over the growth, regeneration and reproduction of biota,
411 with changes in climate associated with an impact on the ability of species to tolerate and
412 respond to disturbance (Enright *et al.*, 2015, Scheffer *et al.*, 2015). The species modelling
413 results indicate a good overall performance of our model based principally on climate input
414 data, highlighting a relatively broad area of suitable climate conditions for the co-occurrence
415 of *Nothofagus gunnii* and *Athrotaxis* spp. (i.e. montane rainforest) in Tasmania. This area is
416 primarily restricted to the mountainous landscape of Tasmania’s west and south (Fig. 1b),
417 where a cool and wet climate is produced by the interaction between topography and
418 orographic rainfall. The apparent failure of montane rainforest to fill all of the available climate
419 space predicted by the model highlights the limitation of this approach for fine-scale mapping
420 and predictive studies, and is attributable to the role of variables such as dispersal limitation,
421 hydrology, geology, aspect, slope, biotic interactions and fire history in determining the local-

422 scale vegetation distribution (Pradervand *et al.*, 2014, Wisz *et al.*, 2013). Nevertheless, our
423 climate-based predictive model allows us to interrogate the role of climate change in
424 determining the response of montane rainforest to disturbance from fire.

425

426 The probability of occurrence determined from climate-based species distribution models has
427 often been interpreted as an indication of how resilient an ecosystem is (Deutsch *et al.*, 2008,
428 Hirota *et al.*, 2011, Huey *et al.*, 2012). Most notably, Hirota *et al.*, (2011) modelled the
429 probability of finding rainforest as a function of mean annual precipitation in the Amazon,
430 concluding that the vast areas of this important forest type that display a low probability of
431 occurrence were low resilience forests at risk of localised extinction following disturbance.

432 Whilst the limitations of SDMs means our model reflects only part of the true niche space of
433 our system, the model allows us interrogate the role of climate in influencing the resilience of
434 this system to fire in the modern landscape. Our model identified areas as having a high
435 probability (>0.5) of occurrence as a function of climate that are spatially restricted to the cool
436 and wet mountain tops in the west and far south (Fig. 2). These areas are likely to foster higher
437 rates of growth and reproduction for montane rainforest trees, relative to areas identified as
438 having low probability of occurrence (<0.5) – i.e. they are high resilience areas. Moreover, the
439 cooler and wetter climate in these high resilience zones are also likely to impact the intensity
440 and severity of fire via the control that climate exerts over fuel moisture content and fire
441 intensity/severity in cool temperate landscapes (Mariani & Fletcher, 2016, McWethy *et al.*,
442 2013, Styger & Kirkpatrick, 2015). In contrast, areas of low probability of occurrence (<0.5)
443 are those that are warmer and/or drier, factors that are likely to negatively impact the growth,
444 recovery and reproduction of montane rainforest species, in turn reducing the ability of
445 montane rainforest to recover from disturbance. Furthermore, these sites will also be more
446 prone to fuel desiccation and fire occurrence.

447

448 **4.2 Climatic change, fire and montane rainforest resilience**

449 Montane rainforest was extant on several mountains across southern Tasmania where it is
450 absent today during the early- to mid-Holocene (ca. 12000-6000 cal yr BP) (Fletcher *et al.*,
451 2018, Macphail, 1980, Macphail, 1979). Further, palaeoecological data indicates that this plant
452 community was able to recover from fire during this time (Fletcher *et al.*, 2018, Fletcher *et al.*,
453 2014; Cadd *et al.*, *in review*). Drawing on this data, Fletcher *et al.* (2018) argue that a broadly
454 stable cool wet climate through early- to mid-Holocene facilitated the post-glacial
455 establishment of montane rainforest across the region and provided conditions in which
456 recovery from fire was possible. The fossil pollen and charcoal data analysed and compiled for
457 our present study indicate that (1) montane rainforest was extant at each of our study sites at
458 ca. 7500 cal yr BP, under the wettest and most stable climate regime of the past 7500 years and
459 (2) that each site experienced some burning after ca. 4000 cal yr BP (Fig. 3). Critically, only
460 the Lake Wilks catchment within the zone of high model-inferred resilience today (0.826) still
461 supports montane rainforest (Table 1). Indeed, while clearly affected by fire, the local montane
462 rainforest at this site displayed a remarkable resilience to burning (Fig. 2). In contrast, the
463 catchments of Owen Tarn (0.437) and Lake Osborne (0.301) within zones of low model-
464 inferred resilience today currently support fire-adapted vegetation. At Lake Osborne, the driest
465 site today, repeated burning between ca. 7500-3000 is followed by recovery of montane
466 rainforest, with an eventual collapse of the forest between ca. 2000-3000 cal yr BP (Fletcher *et*
467 *al.*, 2014). At the substantially wetter Owen Tarn site, montane rainforest also collapsed in
468 response to repeated burning between ca. 2000-3000 cal yr BP, yet, unlike Lake Osborne, the
469 preceding 4000 years were marked by low to absent fire activity and no evidence for an impact
470 of fire on the vegetation. This difference in long-term fire histories between the sites suggests
471 that fire-driven collapse of this forest system is not solely a product of a loss of resilience in

472 response to repeated burning through multiple millennia (*sensu* Fletcher et al., 2014). Rather,
473 it indicates that that fire events under the ‘right’ set of climatic conditions can be sufficient to
474 cause the localised extinction of this community, irrespective of long-term disturbance history.

475

476 The agreement between the model-inferred resilience and the empirical response to fire of
477 montane rainforest at our study sites is consistent with the role of climate in governing both the
478 severity of fire and the ability of vegetation to recover from fire (*sensu* Enright *et al.*, 2015),
479 and supports the use of the climate-based species distribution model as a proxy for resilience
480 to fire in this system. Fires became more frequent in western Tasmania after ca. 4000 cal yr BP
481 (Fig. 2d), a period characterised by a highly variable and overall drier climate over southern
482 Australia (Mariani & Fletcher, 2017, Wilkins *et al.*, 2013). These regional long-term climatic
483 changes likely created unfavourable conditions for post-fire regeneration and growth of *N.*
484 *gunnii* and *Athrotaxis* spp., thus, limiting their ability to recover from fire. Very long-lived
485 species, such as these, can persist *in situ* for extended periods following a shift in climate
486 (Talluto *et al.*, 2017), resulting in a disequilibrium with climate following climatic change
487 (Lenoir & Svenning, 2015, Loehle, 2018). This effect is exacerbated in topographically
488 complex landscapes such as Tasmania where fine scale heterogeneity of microclimates can
489 provide refuge for the persistence of species and communities outside of their broader climate
490 niche (Lenoir *et al.*, 2013). We interpret the pattern of widespread establishment of montane
491 rainforest through the early-mid Holocene (under a wetter climate regime), followed by the
492 subsequent collapse of montane rainforest from OT and LO (low resilience sites) in response
493 to burning, as a consequence of the onset of more variable and drier climatic conditions at the
494 geographic locations in response to regional climatic change over the past ca. 4000 years (Fig.
495 4c). Further, we contend that the extreme longevity of key species in this ecosystem and the
496 complex topography of the region have facilitated the persistence of montane rainforest stands

497 in disequilibrium with climate and at risk of a shift to an alternate fire adapted vegetation state
498 in response to fire (see Fig. 4b for a conceptual representation).

499

500 **4.3 What is the fate of Tasmanian montane rainforests?**

501 Our interpretation of the results of this study imply that large parts of montane rainforest in
502 Tasmania today are either at the limits of their climatic range and/or are in disequilibrium with
503 climate (Fig. 1 and 2). The slow demography of montane rainforest tree species
504 disproportionally exposes them to a disequilibrium with climate following climatic change
505 relative to faster growing trees (Talluto *et al.*, 2017). This situation results in the potential for
506 both a high extinction debt (persistence under unsuitable conditions) and a high colonisation
507 credit (failure to capture new locations) (*sensu* Talluto *et al.*, 2017). Indeed, the extinction risk
508 (Loehle, 2018) for species such as *Athrotaxis* And *N. gunnii* is high, given the potential for
509 climatic change to outpace the ability of species to capture new habitat (Loarie *et al.*, 2009,
510 Loehle, 2018, Talluto *et al.*, 2017). This risk is further heightened in mountainous landscapes
511 and on montane biota, given that steep environmental gradients force rapid response times and
512 there is diminishing availability of habitat upslope in response to global warming (Beniston,
513 2003, Nogués-Bravo *et al.*, 2007, Theurillat & Guisan, 2001). Our contention that long-term
514 climatic change and the slow demography of *Athrotaxis* and *N. gunnii* have fostered a
515 disequilibrium between montane rainforest vegetation and climate, and that this conveys a
516 reduction in resilience to disturbance from fire is significant. Fires are ubiquitous in the
517 Australian landscape and the past ca. 200 years has seen an increase in fire activity in Tasmania
518 that exceeds any point in the past 12000 years (Mariani and Fletcher, 2017). Increased efficacy
519 of lightning as an ignition source, increased human activity and the continual invasion by fire-
520 promoting plants (such as *Eucalyptus*) in to fire-sensitive vegetation all herald a significant
521 threat to the long-term security of this endangered fire-sensitive plant community.

522

523 Fire prevention and mitigation are complex and expensive operations that require a clear
524 strategy. The response to the 2016 wildfires in the Tasmanian highlands, which destroyed large
525 areas of fire-sensitive *Athrotaxis cupressoides*, was largely reactionary due to both the
526 logistical complexities involved in fire management in this remote and rugged region, and the
527 unusual confluence of large-scale lightning storms and a very dry climate (Marris, 2016, Sharp,
528 2016). While our claimed high resilience locations currently act as an important refugium for
529 montane rainforest, continued climatic change will see the gradual erosion of resilience in these
530 areas. Given the difficulties of fire prevention, mitigation and remediation in this very remote
531 and topographically complex landscape, we contend that resource allocation and strategic
532 planning should be invested in fire mitigation strategies that further bolster high resilience sites
533 from potential wildfire, rather than investing in low resilience sites for which the long-term
534 probability of survival is low, even in a scenario of complete fire absence. We argue that similar
535 approaches in other fire sensitive ecosystems that face increasing pressure from a rapidly
536 changing climate and increasing risk of fire might enable a more realistic long-term strategy
537 for survival.

538

539 **ACKNOWLEDGMENTS**

540 Research was supported by ARC grants DI110100019, IN140100050 and AINSE
541 ALNGRA16/024. MM was also supported by an AINSE PGRA scholarship (#12039). We
542 acknowledge that our work was conducted on Tasmanian Aboriginal lands. We thank Laurie
543 Stahle for providing the Lake Wilks charcoal data. We also thank Jane Elith for constructive
544 discussion about MaxEnt modelling. Data for the OT core will be made available on
545 NEOTOMA (<https://www.neotomadb.org/>) upon publication. This is a contribution from the
546 PAGES EcoRe3 Working Group (Workshop 1, Finse, Norway 2017).

547

548 **AUTHOR CONTRIBUTION**

549 MM conceived ideas, elaborated data, performed pollen counts on OT and lead manuscript
550 writing, MSF conceived ideas and edited manuscript text, SH contributed to manuscript
551 editing, HC analysed pollen and charcoal data from Lake Wilks, AZ assisted with 210-Pb
552 dating, GJ assisted with radiocarbon dating.

553

554 **REFERENCES**

- 555 Aldersley A, Murray SJ, Cornell SE (2011) Global and regional analysis of climate and human drivers of
556 wildfire. *Science of the total environment*, **409**, 3472-3481.
- 557 Allen K, Ogden J, Buckley B, Cook E, Baker P (2011) The potential to reconstruct broadscale climate
558 indices associated with southeast Australian droughts from *Athrotaxis* species, Tasmania.
559 *Climate Dynamics*, **37**, 1799-1821.
- 560 Assessment ME (2005) *Ecosystems and Human Well-being: Desertification Synthesis*. World Resources
561 Institute, Washington, DC.
- 562 Baldwin RA (2009) Use of maximum entropy modeling in wildlife research. *Entropy*, **11**, 854-866.
- 563 Barbet-Massin M, Jiguet F, Albert CH, Thuiller W (2012) Selecting pseudo-absences for species
564 distribution models: how, where and how many? *Methods in ecology and evolution*, **3**, 327-
565 338.
- 566 Bateman BL, Pidgeon AM, Radeloff VC, Vanderwal J, Thogmartin WE, Vavrus SJ, Heglund PJ (2016) The
567 pace of past climate change vs. potential bird distributions and land use in the United States.
568 *Global Change Biology*, **22**, 1130-1144.
- 569 Beever EA, Belant JL (2011) 13 Ecological Consequences of Climate Change. *Ecological Consequences
570 of Climate Change: Mechanisms, Conservation, and Management*, 285.
- 571 Beniston M (2003) Climatic change in mountain regions: a review of possible impacts. In: *Climate
572 variability and change in high elevation regions: Past, present & future*. pp Page., Springer.
- 573 Blaauw M (2010) Methods and code for 'classical' age-modelling of radiocarbon sequences.
574 *Quaternary Geochronology*, **5**, 512-518.
- 575 Bond WJ, Woodward FI, Midgley GF (2005) The global distribution of ecosystems in a world without
576 fire. *New Phytologist*, **165**, 525-537.
- 577 Booth TH, Nix HA, Busby JR, Hutchinson MF (2014) BIOCLIM: the first species distribution modelling
578 package, its early applications and relevance to most current MAXENT studies. *Diversity and
579 Distributions*, **20**, 1-9.
- 580 Bowman DMJS (2000) *Australian rainforests: islands of green in a land of fire*, Cambridge, Cambridge
581 University Press.
- 582 Bowman DMJS, Balch JK, Artaxo P *et al.* (2009) Fire in the Earth System. *Science*, **324**, 481-484.
- 583 Brown M (1988) (1988) *Distribution and Conservation of King Billy Pine*. Forestry Commission,
584 Tasmania.
- 585 Burrows MT, Schoeman DS, Richardson AJ *et al.* (2014) Geographical limits to species-range shifts are
586 suggested by climate velocity. *Nature*, **507**, 492.

587 Calais S, Kirkpatrick J (1983) Tree species regeneration after logging in temperate rainforest, Tasmania.
588 In: *Papers and Proceedings of the Royal Society of Tasmania*. pp Page.

589 Calvo E, Pelejero C, De Deckker P, Logan GA (2007) Antarctic deglacial pattern in a 30 kyr record of sea
590 surface temperature offshore South Australia. *Geophysical Research Letters*, **34**.

591 Chen I-C, Hill JK, Ohlemüller R, Roy DB, Thomas CD (2011) Rapid range shifts of species associated with
592 high levels of climate warming. *Science*, **333**, 1024-1026.

593 Cosgrove R (1999) Forty-two degrees south: the archaeology of Late Pleistocene Tasmania. *Journal of*
594 *World Prehistory*, **13**, 357-402.

595 Crimmins SM, Dobrowski SZ, Greenberg JA, Abatzoglou JT, Mynsberge AR (2011) Changes in climatic
596 water balance drive downhill shifts in plant species' optimum elevations. *Science*, **331**, 324-
597 327.

598 Cullen P (1991) Regeneration of *Athrotaxis selaginoides* and other rainforest tree species on landslide
599 faces in Tasmania. pp Page.

600 Cullen PJ (1987) Regeneration patterns in populations on *Athrotaxis selaginoides* D. Don. from
601 Tasmania. *Journal of Biogeography*, **14**, 39 - 51.

602 Cullen PJ, Kirkpatrick JA (1988) The Ecology of *Athrotaxis* D. Don. (Taxodiaceae). I. Stand Structure and
603 Regeneration of *A. cupressoides*. *Australian Journal of Botany*, **36**, 547 - 560.

604 Deutsch CA, Tewksbury JJ, Huey RB, Sheldon KS, Ghalambor CK, Haak DC, Martin PR (2008) Impacts of
605 climate warming on terrestrial ectotherms across latitude. *Proceedings of the National*
606 *Academy of Sciences*, **105**, 6668-6672.

607 Donders TH, Wagner-Cremer F, Visscher H (2008) Integration of proxy data and model scenarios for
608 the mid-Holocene onset of modern ENSO variability. *Quaternary Science Reviews*, **27**, 571-
609 579.

610 Enright NJ, Fontaine JB, Bowman DM, Bradstock RA, Williams RJ (2015) Interval squeeze: altered fire
611 regimes and demographic responses interact to threaten woody species persistence as
612 climate changes. *Frontiers in Ecology and the Environment*, **13**, 265-272.

613 Faegri K, Iversen J (1989) *Textbook of pollen analysis*, New York, Wiley.

614 Fletcher M-S, Benson A, Heijnis H, Gadd PS, Cwynar LC, Rees ABH (2015) Changes in biomass burning
615 mark the onset an ENSO-influenced climate regime at 42°S in southwest Tasmania, Australia.
616 *Quaternary Science Reviews*, **122**, 222-232.

617 Fletcher M-S, Bowman D, Whitlock C, Mariani M, Stahle L (2018) The changing role of fire in conifer-
618 dominated temperate rainforest through the last 14,000 years. *Quaternary Science Reviews*,
619 **182**, 37-47.

620 Fletcher M-S, Moreno PI (2012) Have the Southern Westerlies changed in a zonally symmetric manner
621 over the last 14,000 years? A hemisphere-wide take on a controversial problem. *Quaternary*
622 *International*, **253**, 32-46.

623 Fletcher M-S, Thomas I (2010) The origin and temporal development of an ancient cultural landscape.
624 *Journal of Biogeography*, **37**, 2183-2196.

625 Fletcher M-S, Wolfe BB, Whitlock C *et al.* (2014) The legacy of mid Holocene fire on a Tasmanian
626 montane landscape. *Journal of Biogeography*.

627 Harris R, Beaumont L, Vance T *et al.* (2018) Biological responses to the press and pulse of climate
628 trends and extreme events. *Nature Climate Change*, **8**, 579.

629 Harris S, Kitchener A (eds) (2005) *From forest to fjaldmark : descriptions of Tasmania's vegetation*,
630 Hobart, Department of Primary Industries, Water and Environment.

631 Hennessy K, Lucas C, Nicholls N, Bathols J, Suppiah R, Ricketts J (2005) Climate change impacts on fire-
632 weather in south-east Australia. In: *Climate Impacts Group, CSIRO Atmospheric Research and*
633 *the Australian Government Bureau of Meteorology, Aspendale*. pp Page.

634 Hijmans RJ, Phillips S, Leathwick J, Elith J, Hijmans MRJ (2017) Package 'dismo'. *Circles*, **9**.

635 Hill RS (1991) Tertiary Nothofagus (Fagaceae) macrofossils from Tasmania and Antarctica and their
636 bearing on the evolution of the genus. *Botanical Journal of the Linnean Society*, **105**, 73-112.

637 Hill RS, Jordan GJ, Macphail MK (2015) Why we should retain *Nothofagus sensu lato*. Australian
638 Systematic Botany, **28**, 190-193.

639 Hirota M, Holmgren M, Van Nes EH, Scheffer M (2011) Global resilience of tropical forest and savanna
640 to critical transitions. Science, **334**, 232-235.

641 Hodgson DA, Vyverman W, Chepstow-Lusty A, Tyler P (2000) From rainforest to wasteland in 100
642 years: The limnological legacy of the Queenstown mines, Western Tasmania. Archive
643 Hydrobiologique, **149**, 153 - 176.

644 Hogg AG, Hua Q, Blackwell PG *et al.* (2013) SHCal13 Southern Hemisphere calibration, 0–50,000 cal yr
645 BP. Radiocarbon.

646 Holz A, Wood SW, Veblen TT, Bowman DM (2014) Effects of high severity fire drove the population
647 collapse of the subalpine Tasmanian endemic conifer *Athrotaxis cupressoides*. Global Change
648 Biology.

649 Huey RB, Kearney MR, Krockenberger A, Holtum JA, Jess M, Williams SE (2012) Predicting organismal
650 vulnerability to climate warming: roles of behaviour, physiology and adaptation. Phil. Trans.
651 R. Soc. B, **367**, 1665-1679.

652 Kirkpatrick JB, Dickinson KJM (1984) The impact of fire on Tasmanian alpine vegetation and soils.
653 Australian Journal of Botany, **32**, 613-629.

654 Kumar S, Spaulding SA, Stohlgren TJ, Hermann KA, Schmidt TS, Bahls LL (2009) Potential habitat
655 distribution for the freshwater diatom *Didymosphenia geminata* in the continental US.
656 Frontiers in Ecology and the Environment, **7**, 415-420.

657 Kumar S, Stohlgren TJ (2009) Maxent modeling for predicting suitable habitat for threatened and
658 endangered tree *Canacomyrica monticola* in New Caledonia. Journal of Ecology and the
659 Natural Environment, **1**, 094-098.

660 Lenoir J, Graae BJ, Aarrestad PA *et al.* (2013) Local temperatures inferred from plant communities
661 suggest strong spatial buffering of climate warming across Northern Europe. Global Change
662 Biology, **19**, 1470-1481.

663 Lenoir J, Svenning JC (2015) Climate-related range shifts—a global multidimensional synthesis and new
664 research directions. Ecography, **38**, 15-28.

665 Loarie SR, Duffy PB, Hamilton H, Asner GP, Field CB, Ackerly DD (2009) The velocity of climate change.
666 Nature, **462**, 1052-U1111.

667 Loehle C (2018) Disequilibrium and relaxation times for species responses to climate change.
668 Ecological modelling, **384**, 23-29.

669 Macphail M (1980) Regeneration processes in Tasmanian forests—a long-term perspective based on
670 pollen analysis [management implications]. Search, **11**, 184-190.

671 Macphail MK (1979) Vegetation and climates in southern Tasmania since the last glaciation.
672 Quaternary Research, **11**, 306-341.

673 Marcott SA, Shakun JD, Clark PU, Mix AC (2013) A reconstruction of regional and global temperature
674 for the past 11,300 years. Science, **339**, 1198-1201.

675 Mariani M, Connor SE, Fletcher MS *et al.* (2017) How old is the Tasmanian cultural landscape? A test
676 of landscape openness using quantitative land-cover reconstructions. Journal of
677 Biogeography, **44**, 2410-2420.

678 Mariani M, Fletcher M-S (2017) Long-term climate dynamics in the extra-tropics of the South Pacific
679 revealed from sedimentary charcoal analysis. Quaternary Science Reviews, **173**, 181-192.

680 Mariani M, Fletcher MS (2016) The Southern Annular Mode determines inter-annual and centennial-
681 scale fire activity in temperate southwest Tasmania, Australia. Geophysical Research Letters,
682 **43**, 1702–1709.

683 Mariani M, Holz A, Veblen TT, Williamson G, Fletcher MS, Bowman DM (2018) Climate change
684 amplifications of climate-fire teleconnections in the Southern Hemisphere. Geophysical
685 Research Letters, **45**, 5071-5081.

686 Marris E (2016) Tasmanian bushfires threaten iconic ancient forests. Nature, **530**, 137.

687 Mcwethy D, Higuera P, Whitlock C *et al.* (2013) A conceptual framework for predicting temperate
688 ecosystem sensitivity to human impacts on fire regimes. *Global Ecology and Biogeography*,
689 **22**, 900-912.

690 Moy CM, Seltzer GO, Rodbell DT, Anderson DM (2002) Variability of El Nino/Southern Oscillation
691 activity at millennial timescales during the Holocene. *Nature*, **420**, 162-165.

692 Nix HA (1986) A biogeographic analysis of Australian elapid snakes. *Atlas of elapid snakes of Australia*,
693 **7**, 4-15.

694 Nogués-Bravo D, Araújo MB, Errea M, Martínez-Rica J (2007) Exposure of global mountain systems to
695 climate warming during the 21st Century. *Global Environmental Change*, **17**, 420-428.

696 Ogden J (1978) Investigations of the dendrochronology of the genus *Athrotaxis* D. Don (Taxodiaceae)
697 in Tasmania. *Tree-Ring Bulletin*.

698 Parmesan C (2006) Ecological and evolutionary responses to recent climate change. *Annu. Rev. Ecol.*
699 *Evol. Syst.*, **37**, 637-669.

700 Parmesan C, Yohe G (2003) A globally coherent fingerprint of climate change impacts across natural
701 systems. *Nature*, **421**, 37.

702 Phillips SJ, Dudík M, Schapire RE (2004) A maximum entropy approach to species distribution
703 modeling. In: *Proceedings of the twenty-first international conference on Machine learning*.
704 pp Page, ACM.

705 Ramsey CB (2009) Bayesian analysis of radiocarbon dates. *Radiocarbon*, **51**, 337-360.

706 Rees AB, Cwynar LC, Fletcher M-S (2015) Southern Westerly Winds submit to the ENSO regime: A
707 multiproxy paleohydrology record from Lake Dobson, Tasmania. *Quaternary Science Reviews*,
708 **126**, 254-263.

709 Scheffer M, Barrett S, Carpenter S *et al.* (2015) Creating a safe operating space for iconic ecosystems.
710 *Science*, **347**, 1317-1319.

711 Seidl R, Rammer W, Spies TA (2014) Disturbance legacies increase the resilience of forest ecosystem
712 structure, composition, and functioning. *Ecological Applications*, **24**, 2063-2077.

713 Seidl R, Spies TA, Peterson DL, Stephens SL, Hicke JA (2016) Searching for resilience: addressing the
714 impacts of changing disturbance regimes on forest ecosystem services. *Journal of Applied*
715 *Ecology*, **53**, 120-129.

716 Sharp N (2016) Lightning strikes and climate change. *Arena Magazine* (Fitzroy, Vic), 13.

717 Stahle LN, Chin H, Haberle S, Whitlock C (2017) Late-glacial and Holocene records of fire and
718 vegetation from Cradle Mountain National Park, Tasmania, Australia. *Quaternary Science*
719 *Reviews*, **177**, 57-77.

720 Stephens SL, Burrows N, Buyantuyev A *et al.* (2014) Temperate and boreal forest mega-fires:
721 characteristics and challenges. *Frontiers in Ecology and the Environment*, **12**, 115-122.

722 Styger J, Kirkpatrick JB (2015) Less than 50 millimetres of rainfall in the previous month predicts fire
723 in Tasmanian rainforest. In: *Papers and Proceedings of the Royal Society of Tasmania*. pp Page.

724 Talluto MV, Boulangeat I, Vissault S, Thuiller W, Gravel D (2017) Extinction debt and colonization credit
725 delay range shifts of eastern North American trees. *Nature Ecology & Evolution*, **1**, 0182.

726 Team RCD (2013) R: A language and environment for statistical computing. In: *R Foundation for*
727 *Statistical Computing* pp Page, Vienna Austria.

728 Theurillat J-P, Guisan A (2001) Potential impact of climate change on vegetation in the European Alps:
729 a review. *Climatic Change*, **50**, 77-109.

730 Vanderwal J, Murphy HT, Kutt AS, Perkins GC, Bateman BL, Perry JJ, Reside AE (2013) Focus on
731 poleward shifts in species' distribution underestimates the fingerprint of climate change.
732 *Nature Climate Change*, **3**, 239.

733 Westerling AL, Hidalgo HG, Cayan DR, Swetnam TW (2006) Warming and earlier spring increase
734 western US forest wildfire activity. *Science*, **313**, 940-943.

735 Whitlock C, Colombaroli D, Conedera M, Tinner W (2017) Land-use history as a guide for forest
736 conservation and management. *Conservation Biology*.

- 737 Whitlock C, Larsen CPS (2001) Charcoal as a fire proxy. Tracking environmental change using lake
738 sediments. pp Page, Kluwer Academic Publishers, Dordrecht, The Netherlands.
- 739 Wilkins D, Gouramanis C, De Deckker P, Fifield LK, Olley J (2013) Holocene lake-level fluctuations in
740 Lakes Keilambete and Gnotuk, southwestern Victoria, Australia. *The Holocene*, **23**, 784-795.
- 741 Willis KJ, Birks HJB (2006) What is natural? The need for a long-term perspective in biodiversity
742 conservation. *Science*, **314**, 1261.
- 743 Wood SW, Murphy BP, Bowman DM (2011) Firescape ecology: how topography determines the
744 contrasting distribution of fire and rain forest in the south-west of the Tasmanian Wilderness
745 World Heritage Area. *Journal of Biogeography*, **38**, 1807-1820.
- 746 Xia Y, Zhao J, Collerson KD (2001) Early-Mid Holocene climatic variations in Tasmania, Australia: multi-
747 proxy records in a stalagmite from Lynds Cave. *Earth and Planetary Science Letters*, **194**, 177-
748 187.

749

750

751

SUPPORTING INFORMATION

752

753 **Climate change reduces resilience to fire in subalpine rainforests**

754 Michela Mariani^{1,2*}, Michael-Shawn Fletcher^{*1}, Simon Haberle³, Hahjung Chin³, Zawadzki, A.⁴,

755 Geraldine Jacobsen⁴

756 ¹School of Geography, University of Melbourne, VIC, Australia

757 ² School of Geography, University of Nottingham, Nottingham, United Kingdom

758 ³ Department of Archaeology and Natural History, the Australian National University, ACT, Australia

759 ⁴ Australian Nuclear Science and Technology Organisation (ANSTO), NSW, Australia

760 *Corresponding authors

761

762 SUPPORTING INFORMATION CAPTIONS

763 **Fig. S1** Maps showing the bioclim variables used to run the MaxEnt model.

764 **Fig. S2** Matrix showing biplots of the bioclim variables.

765 **Fig. S3** Maps showing the location of the data points used for a) training dataset and b)
766 testing dataset. Presences and pseudo-absences are shown (see legend).

767 **Fig. S4** Graph showing the contribution of bioclim variables in the MaxEnt model run.

768 **Fig. S5** Response curves based on presence data of the bioclim variables.

769 **Fig. S6** Response curves based on presence and pseudo-absence data of the bioclim variables.

770 **Fig. S7** Model evaluation results for a) training and b) testing datasets used for MaxEnt (data
771 points shown in Figure S3).

772 **Fig. S8** Modern climate space for montane rainforest in Tasmania using the two climatic
773 variables with the highest contribution in MaxEnt (bio10 and bio18, respectively). Colour
774 code indicates the MaxEnt value ranges.

775 **Table S1a** Table with the radiocarbon dates obtained on the Owen Tarn core (OT-1).

776 **Table S1b** Table showing the results of ²¹⁰Pb dating on the Owen Tarn core (OT-1).

777 **Fig. S9** Age-depth model for the Owen Tarn core (OT-1) obtained with OxCal 4.2 (Ramsey,
778 2009).

779 **Fig. S10** Age-depth models for **a)** Lake Osborne (LO-2; Fletcher *et al.*, 2018) and **b)** Lake
780 Wilks (LW-3; Stahle *et al.*, 2017).

781

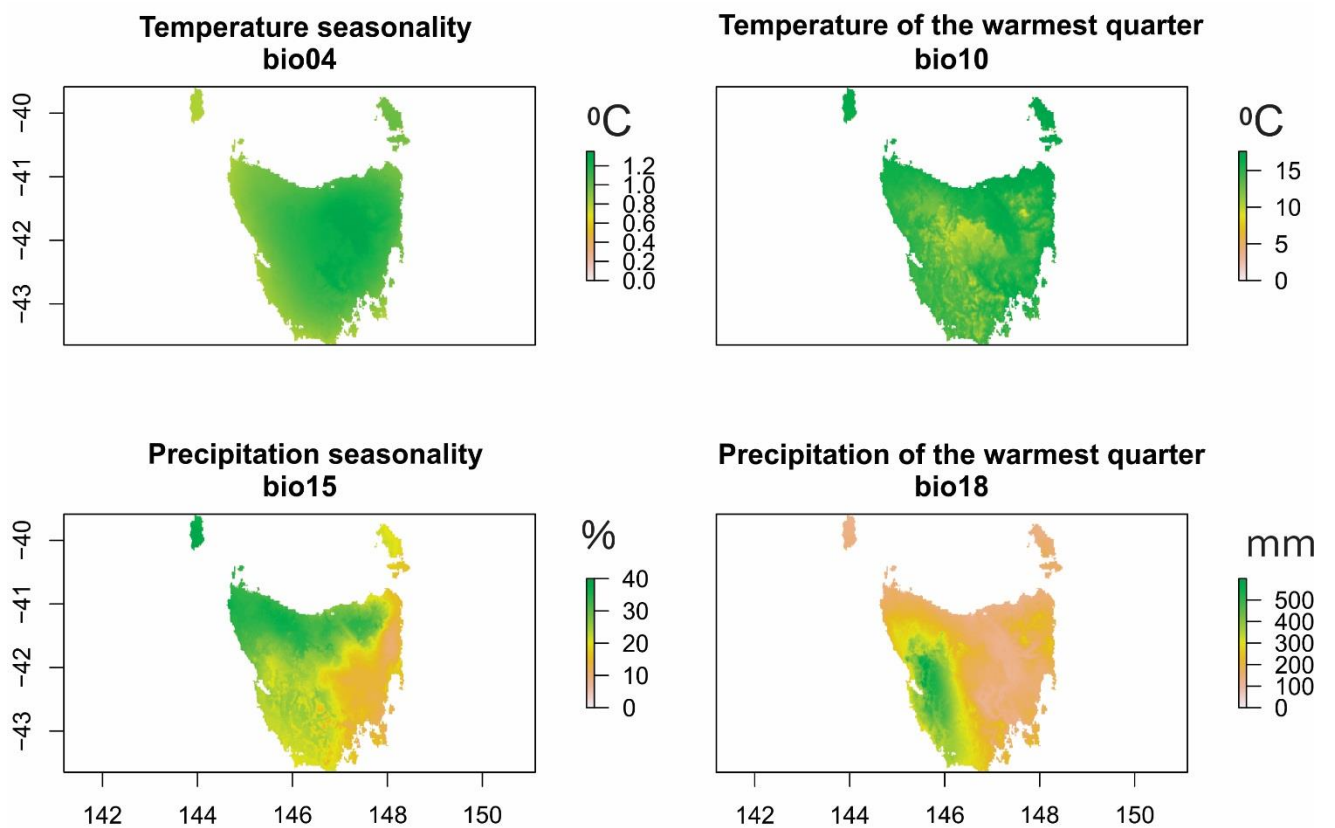
782 Additional supporting information files:

783 A) Map of the co-occurrence points “Co_occurrence points_suppinfo.kmz” (Google
784 Earth)

785 B) Map of the SDM output for this study “MaxEnt_suppinfo.kmz” (Google Earth)

786

787 **Fig. S1** Maps showing the bioclim variables used to run the MaxEnt model.



788

789

790

791

792

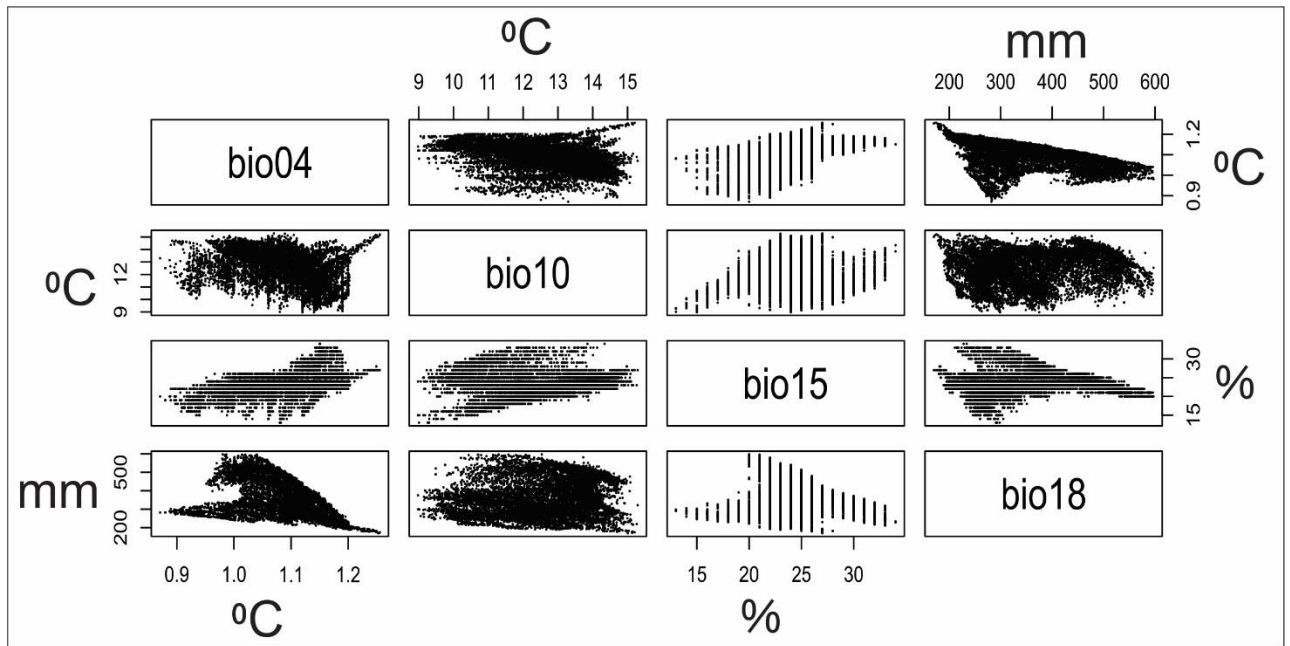
793

794

795

796

797 **Fig. S2** Matrix showing biplots of the bioclim variables.

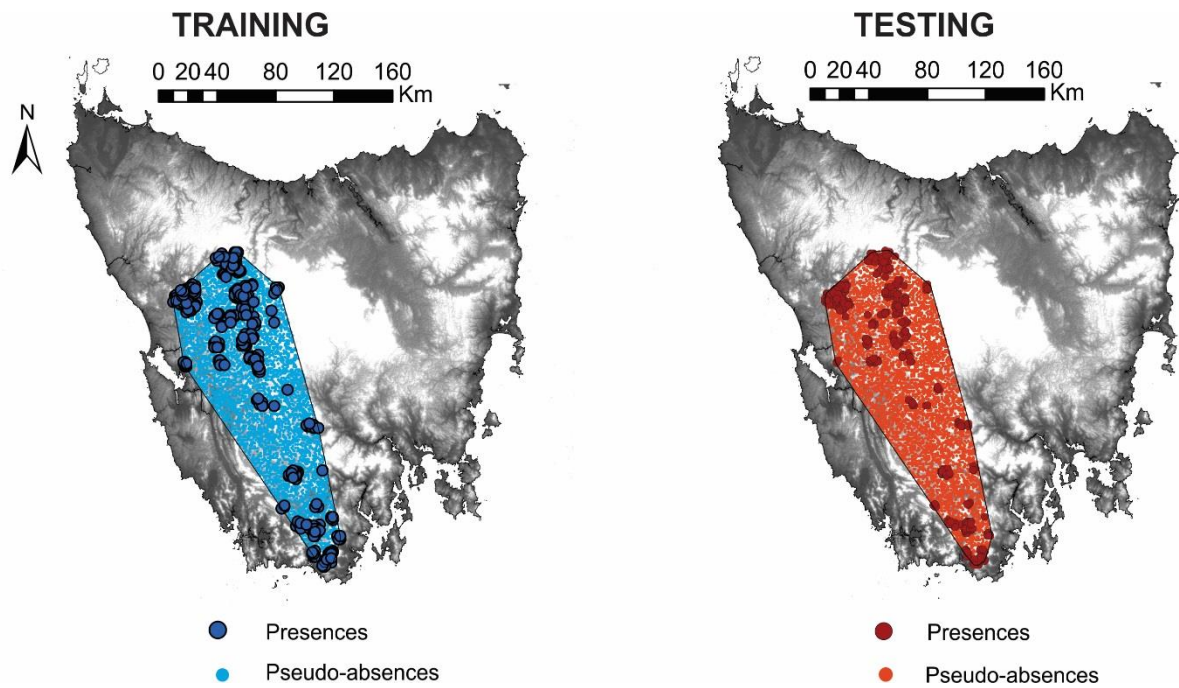


798

799

800

801 **Fig. S3** Maps showing the location of the data points used for a) training dataset and b)
802 testing dataset. Presences and pseudo-absences are shown (see legend).

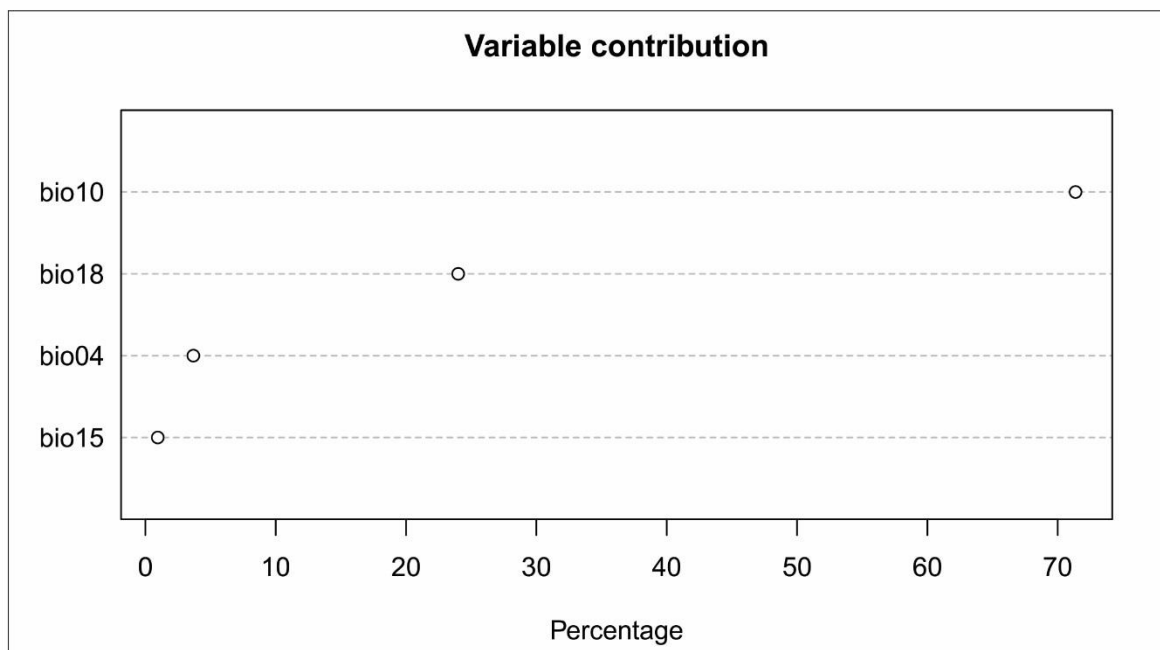


803

804

805

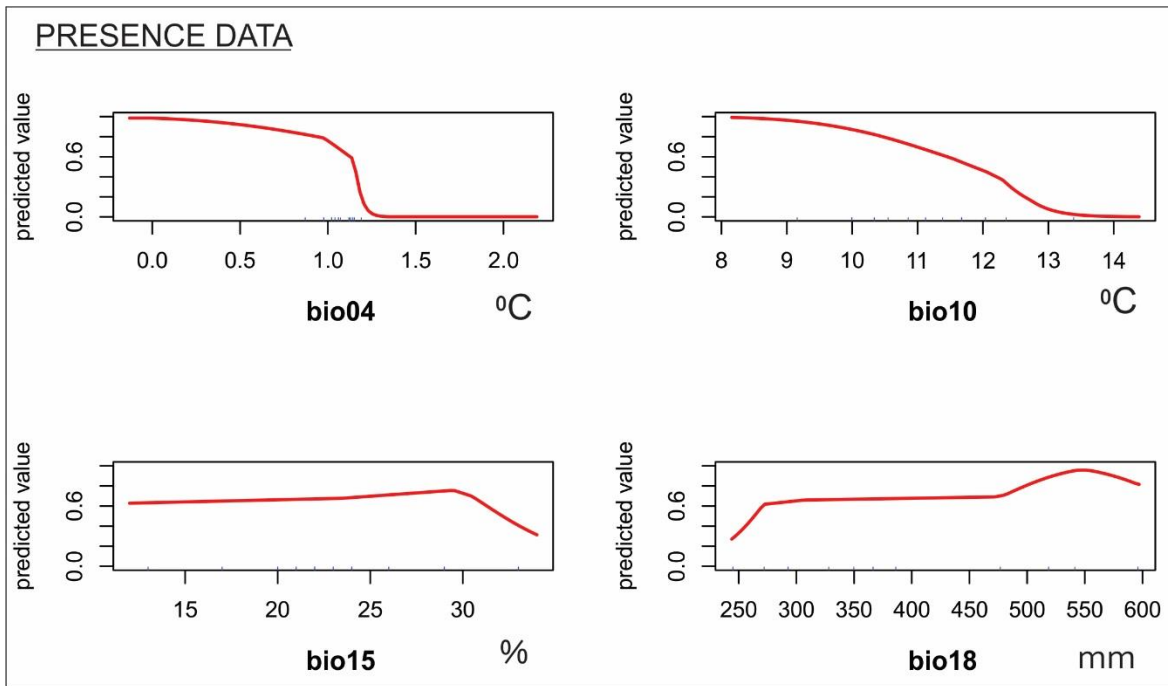
806 **Fig. S4** Graph showing the contribution of bioclim variables in the MaxEnt model run.



807

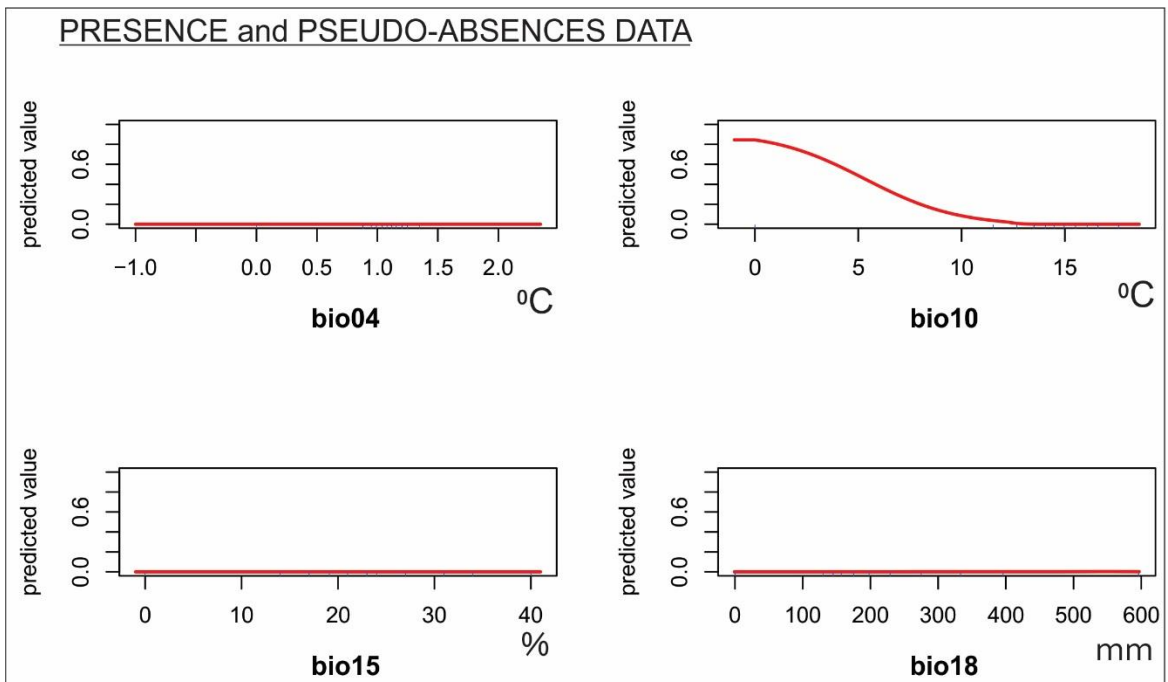
808

809 **Fig. S5** Response curves based presence data of the bioclim variables.



810

811 **Fig. S6** Response curves based on presence and pseudo-absence data of the bioclim variables.

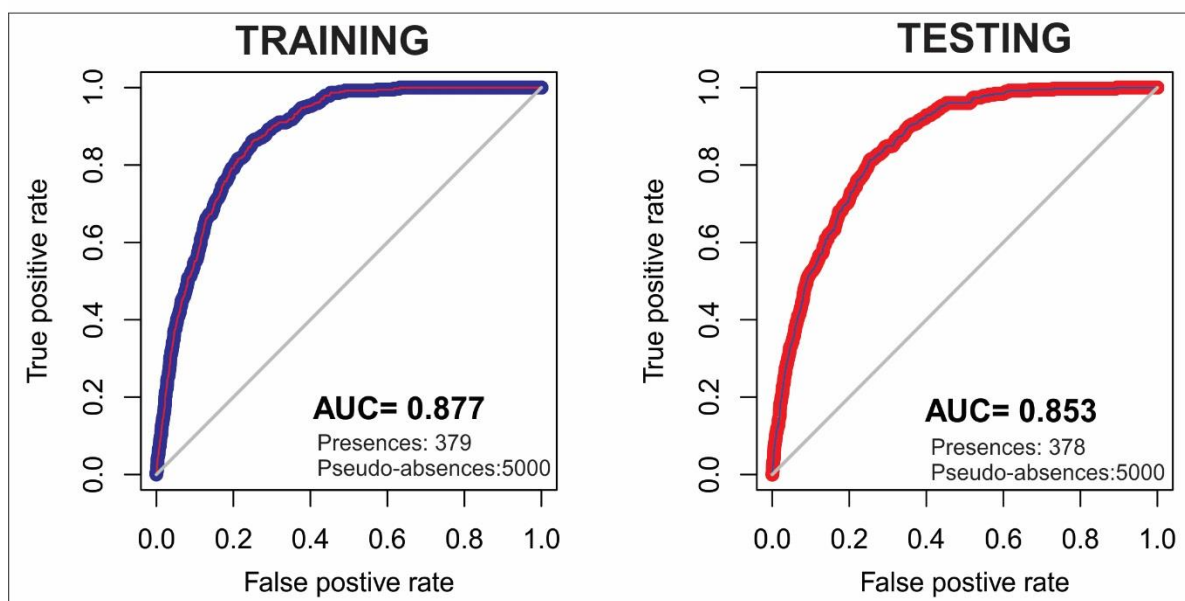


812

813

814

815 **Fig. S7** Model evaluation results for a) training and b) testing datasets used for MaxEnt (data
816 points shown in Fig. S3).



817

818

819 **Table S1a** Table with the radiocarbon dates obtained on the Owen Tarn core (OT-1).

SAMPLE code	LAB code	Depth (cm)	Material dated	¹⁴ C age	Error (yrs)	Upper cal BP (2σ)	Lower cal BP (2σ)	Median age (cal BP)
TAS1501 - RC1	OZU876	18.25	Bulk sediment	790	40	739	571	686
TAS1501 - RC2	D-AMS 015343	24.75	Bulk sediment	1402	25	1311	1188	1286
TAS1501 - RC3	OZU232	27.75	Bulk sediment	1880	35	1874	1702	1777
TAS1501 - RC4	D-AMS 010821	34.25	Bulk sediment	2300	28	2348	2160	2247
TAS1501 - RC5	D-AMS 015344	40.25	Bulk sediment	2904	24	3073	2873	2978
TAS1501 - RC6	D-AMS 010822	45.75	Bulk sediment	3332	26	3608	3446	3516
TAS1501 - RC7	OZU877	50.25	Bulk sediment	5050	60	5902	5611	5750
TAS1501 - RC8	OZU233	53.75	Bulk sediment	5515	35	6393	6188	6276
TAS1501 - RC9	D-AMS 010823	65.25	Bulk sediment	6465	31	7422	7276	7357
TAS1501 - RC10	D-AMS 015345	67.75	Bulk sediment	6537	34	7482	7316	7401
TAS1501 - RC11 *	OZU878	67.75	Bulk sediment	7810	60	8700	8410	8543

820

821

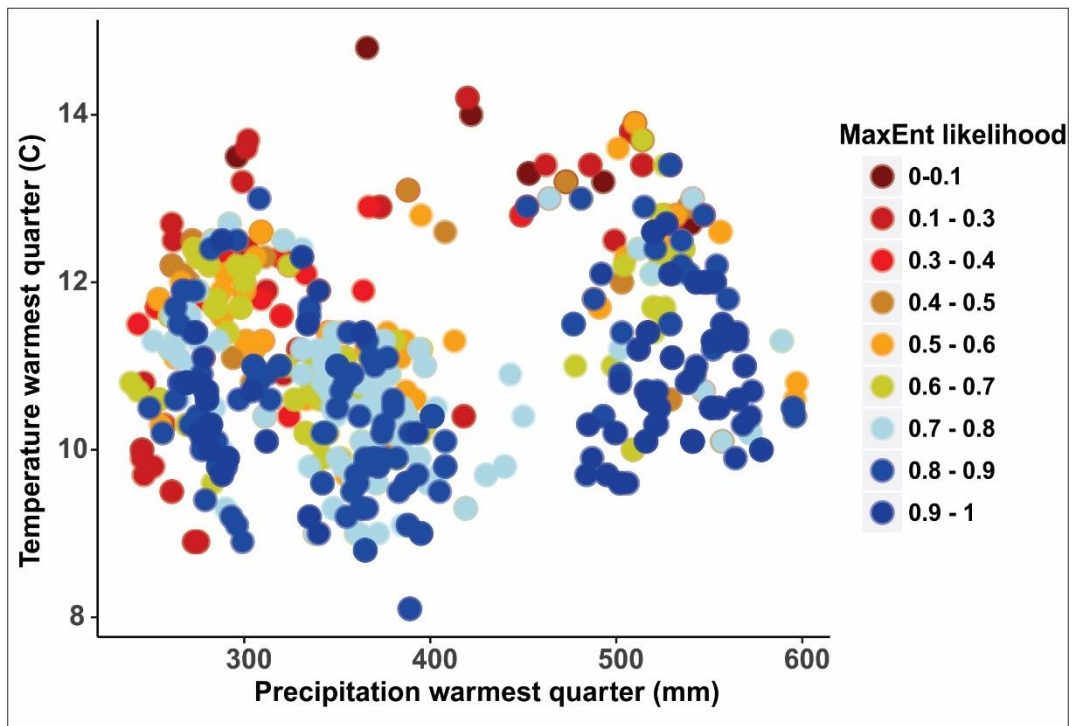
822 **Table S1b** Table showing the results of ²¹⁰Pb dating on the Owen Tarn core (OT-1).

SAMPLE code	LAB code	Depth (cm)	Material dated	CRS model Mass Accumulation Rates (g/cm ² /year)			CRS age (yrs BP)	CRS age error (yrs)
					±			
TAS1501 - LD1	S385	0.25	Bulk sediment (sieved <63μm)	0.07	±	0.00	-63	2
TAS1501 - LD2	S386	1.25	Bulk sediment (sieved <63μm)	0.23	±	0.03	-56	3
TAS1501 - LD3	S387	3.75	Bulk sediment (sieved <63μm)	0.48	±	0.08	-48	4
TAS1501 - LD4	S388	5.25	Bulk sediment (sieved <63μm)	0.23	±	0.03	-43	5
TAS1501 - LD5	S389	11.75	Bulk sediment (sieved <63μm)	0.08	±	0.02	-5	8
TAS1501 - LD6	S390	14.25	Bulk sediment (sieved <63μm)	0.07	±	0.02	17	9

823

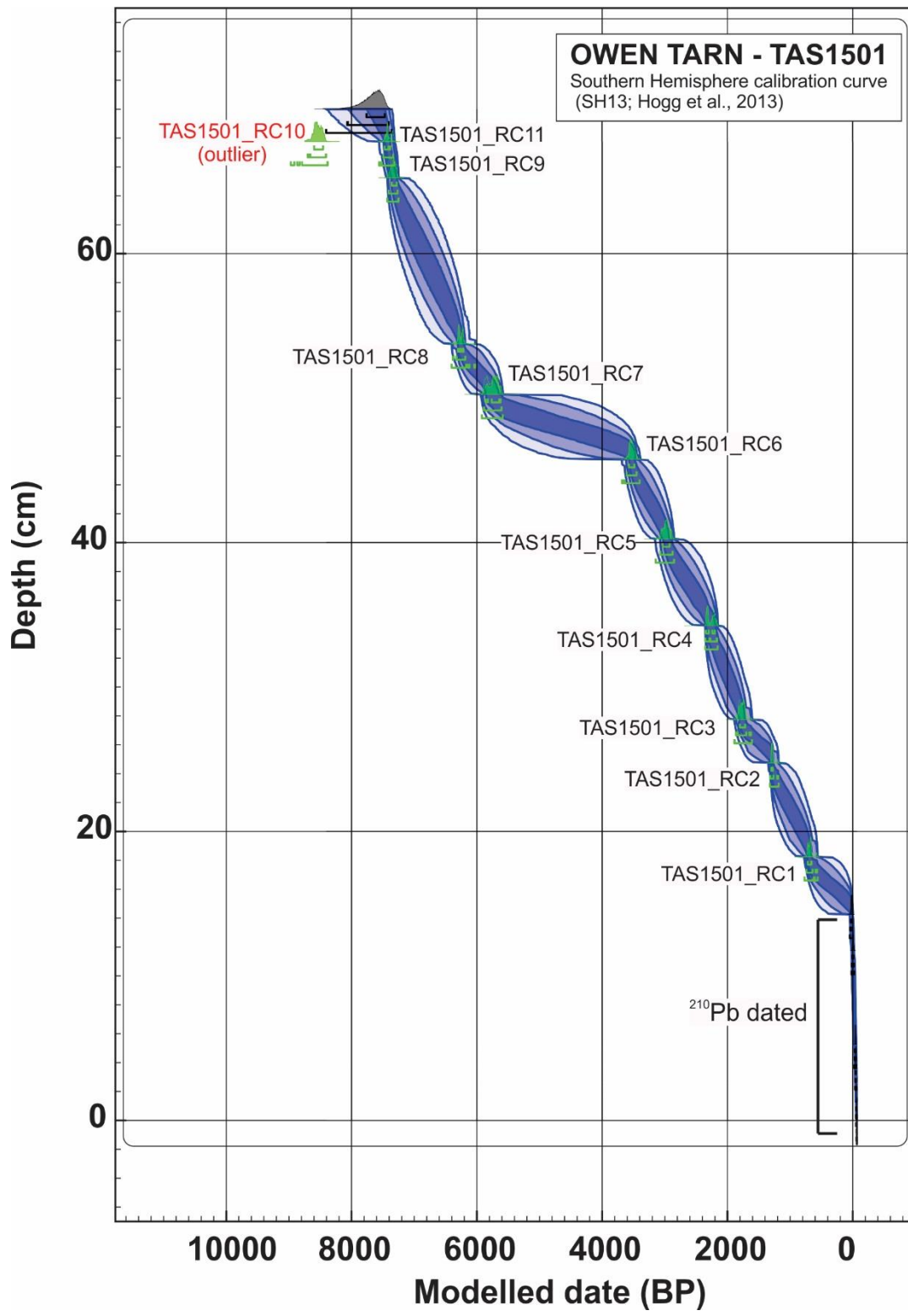
824

825 **Fig. S8** Modern climate space for montane rainforest in Tasmania using the two climatic
826 variables with the highest contribution in MaxEnt (bio10 and bio18, respectively). Colour
827 code indicates the MaxEnt value ranges.



828

829 **Fig. S9** Age-depth model for the Owen Tarn core (OT-1) obtained with OxCal 4.2 (Ramsey,
830 2009).

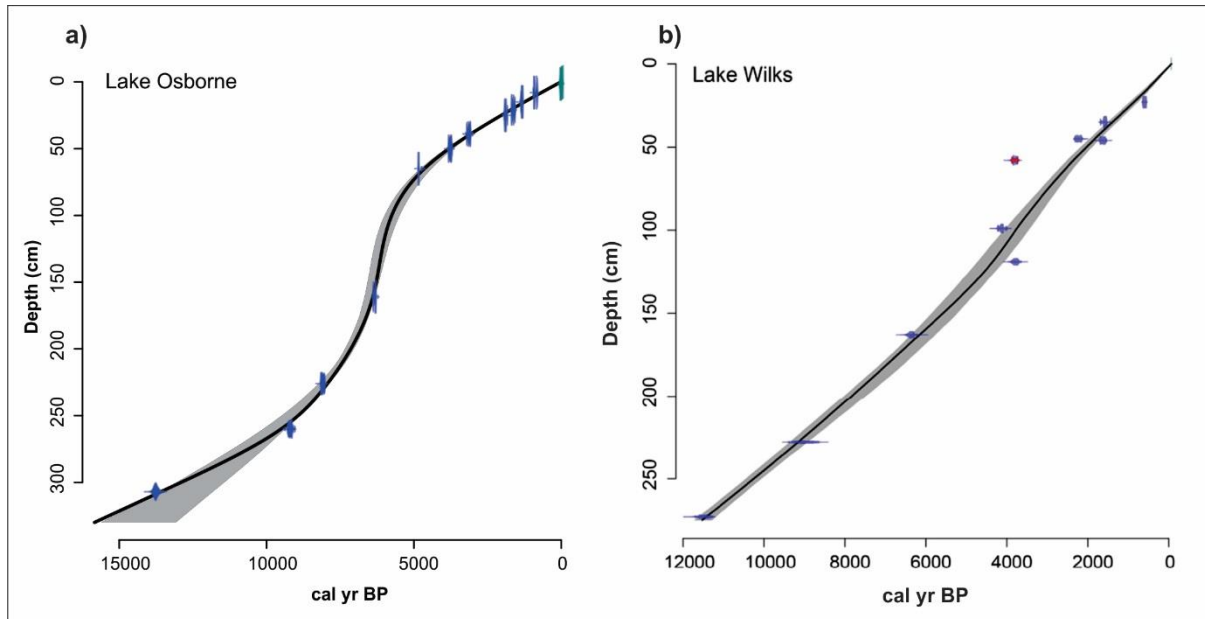


831

832

833 **Fig. S10** Age-depth models for **a)** Lake Osborne (LO-2; Fletcher *et al.*, 2018) and **b)** Lake
834 Wilks (LW-3; Stahle *et al.*, 2017).

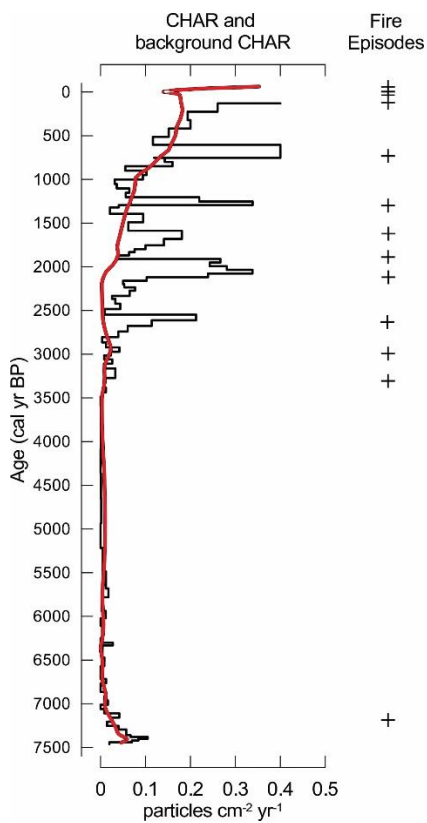
835



836

837

838 **Fig. S11** Charcoal accumulation rates (CHAR), background charcoal and fire events detected
839 by CharAnalysis (Higuera, 2009) on the Owen Tarn sequence.



840